# Enhancing Oil Sands Tailings Treatment by Lime Addition

by

Yang Tan

A thesis submitted in partial fulfillment of the requirements for the degree of

Master of Science

In

Chemical Engineering

Department of Chemical and Materials Engineering
University of Alberta

# Abstract

This research aims to improve oil sands tailings treatment by applying a combination of quick lime (calcium oxide) and anionic or cationic polymers in the flocculation process. A procedure including mixing lime, dilution of mature fine tailings (MFT) in the lime supernatant and addition of polymeric flocculants optimizes settling efficiency of MFT solids. An improvement of flocculation is obtained as shown by achieving significantly higher initial settling rate, lower turbidity of recycled water and higher solid content sediments with less amount of polymers. Both anionic polymer Magnafloc336 and cationic polymer Zetag8110 are tested separately.

In order to study the mechanism and explain why the best performance appears with the intermediate dosage of lime, focus beam reflectance measurement (FBRM) is applied to observe the floc size change during the flocculation process. Zeta potentials of tailings particles are measured by zeta phoremeter in solutions of different ion concentrations and pH. The results together with settling test results and ion chromatography measurements are analyzed. We find that the increased concentration of calcium monohydroxide ions ($Ca(OH)^+$) is the key species influencing zeta potentials of tailings particles and flocculation process. Finally, quartz crystal microbalance with dissipation monitoring (QCMD) is applied study the adsorption mechanism and conformational changes of polymers on tailings particles. We find that increasing the lime concentration can enhance the adsorption of both anionic and cationic polymers.

The increased calcium ions and hydrolyzed ions are shown to reduce the negative charges of the particle surface and also screen the strong repulsions between segments of polymer chains. The conformational changes of polymers are detected by dissipation monitoring on QCMD. The more compact conformations of polymers may facilitate the adsorption but could also hinder the

bridging effect of flocculation process. With excessive concentrations of lime, we observe a decay of flocculation performance.

## Acknowledgement

I would like to thank Professor Zhenghe Xu for his kindly guidance and professional advice throughout my whole program. I have learned much about not only the research, but also the dedicated and optimistic attitude towards work and life from him. I also would like to give credits to Mr. Jim Skwarok, Ms. Jie Ru, Ms. Lisa Carreiro and Ms. Ni Yang who helped me so much on the lab equipment, safety and communications with Professor Xu.

I have my sincere gratitude to Dr. Chen Wang as a senior peer who guided me every step about tailings treatment in the lab from the beginning of my project. I appreciate that Dr. Rogerio Manica, Mr. Yi Lu, Dr. Zuoli Li, Mr. Jason Ng and all the other group members are willing to help me throughout the challenges I met during these years. I could not accomplish my program without their kindness.

# Table of Contents

# List of Figures

# List of Tables

# Chapter 1 Introduction

## 1.1 Basics of Oil Sands

The Athabasca Oil Sands contains a vast amount of crude bitumen, an unconventional resource of hydrocarbon, which is considered as the second largest oil reserves in the world (Masliyah et al, 2011). It is estimated to contain 174.4 billion bbl of oil from oil sands reserve as compared with 4.5 billion bbl for conventional crude oil reserves in Canada (Radler, 2003). For year 2015, Canada produced 4485 thousand bbl of oil daily, which is 4.9% of the total world production after US, Saudi Arabia and Russia (BP Global, 2016). Among this crude oil production, more than 50% came from oil sands and the estimated ratio will be 75% in 2025 (CAPP, 2014). Needless to say, the oil sands industry is vital to Canadian economy and worldwide energy security.

Since the first time crude oil was extracted commercially from oil sands by Suncor in 1967, the oil sands industry has been growing vastly till now (Figure 1.1). Meanwhile, the industry draws public attentions due to environmental influence by mining and upgrading process, especially the harmful by-product such as oil sands tailings from open pit mining operations. The growth of its volume – the oil sands ponds has also been exponential (Figure 1.2). Advanced technologies are urged to stop its rapid expansion in a short period of time.

This chapter introduces the origin of oil sands, the basic procedures of extracting crude oil (aeration, flotation and froth treatment), the source of oil sands tailings and conventional routines of tailings treatment. As the following some advanced mining technologies which can avoid tailings production are introduced. At last the objective and organization of this research are displayed.

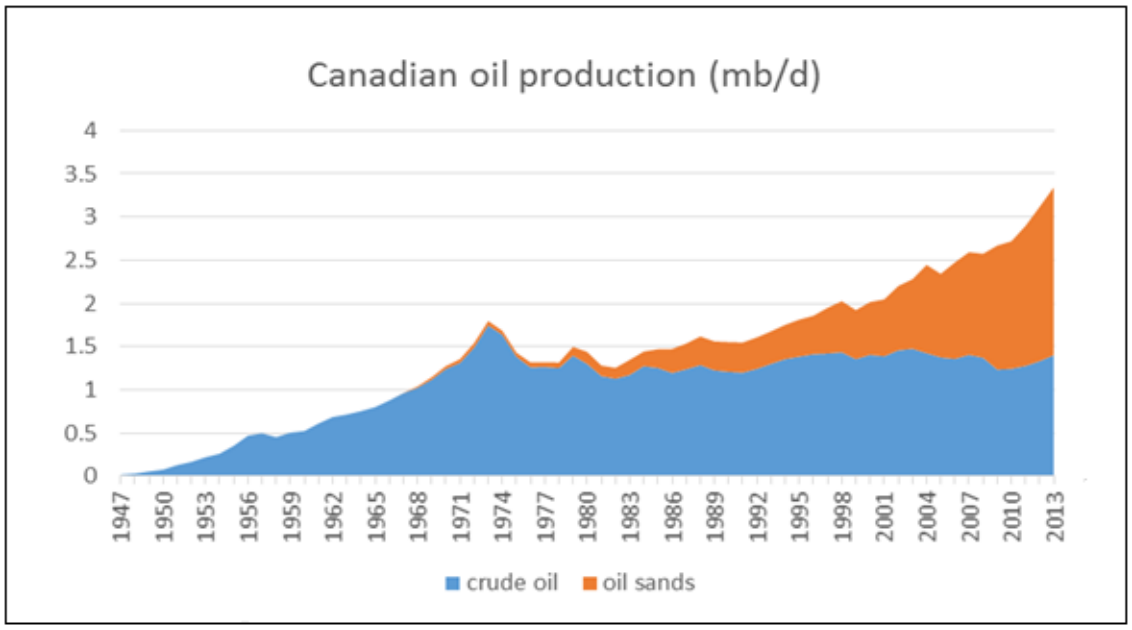


**Figure 1.1 Comparison of oil sands and crude oil production of Canada (Hamilton, 2014)**

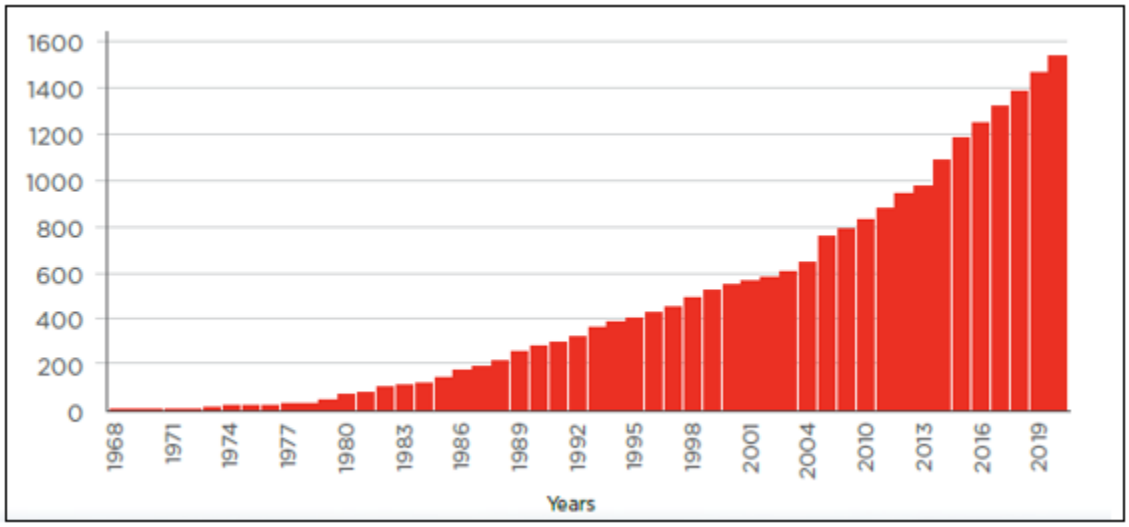


**Figure 1.2 Total volume of oil sands tailings ($Mm^3$) in 50 years (NRDC, 2017)**

1.2 Composition of Oil Sands

It is widely believed that oil sands were formed from marine organisms transformed by the high temperature and pressure under the ancient sea. The light hydrocarbon is consumed by bacteria and the heavy hydrocarbon (main component) remains mixed with solids and water (Figure 1.3).

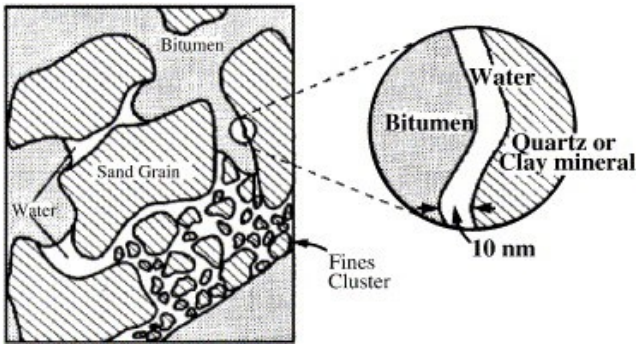


**Figure 1.3 Sketch of oil sands structure (Takamura, 1982)**

The composition of oil sands varies among different reserves and depths. Typically, it can contain 10% bitumen, 5% water and 85% solids (Masliyah, 2012). Among the solids, the particle size can vary from submicron level to millimeter level. The composition of solids has a vast influence on the performance of oil sands processing. Mineral solids smaller than 44μm is defined as *fines* and 2μm as *clays* by oil sands industry. More fines and clays usually result in detrimental effects on bitumen recovery, froth treatment and tailing treatment because of their special interactions with bitumen, air bubbles, minerals and polymers.

## 1.3 Open Pit Mining

To extract the bituminous component from oil sands ores, there are mainly 2 types of technologies: open pit mining which is applied to relatively shallow level deposits less than 65 m in depth and in-situ recovery applied to ores which are deeper underground. Open pit mining is the conventional way of majority recovery, although in-situ operations have surpassed in recent years (Figure 1.4).

Producing bitumen by open pit mining requires 3 opertions after mining and crushing the ores: extraction, froth treatment and tailing treatment (Figure 1.5).

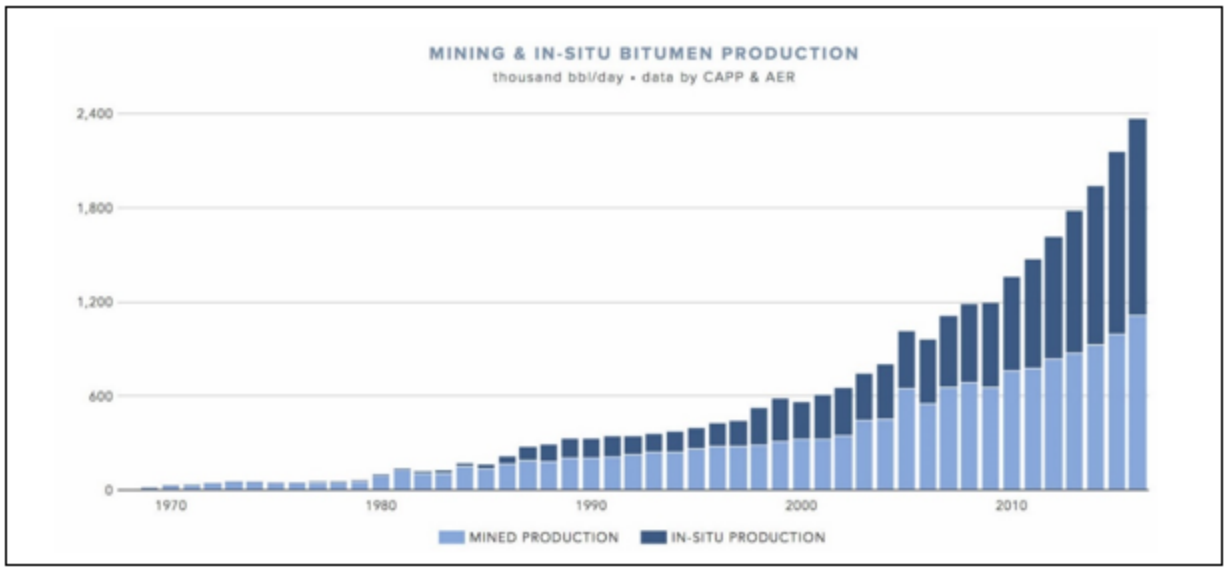


**Figure 1.4 Mining and in-situ bitumen production rate (Oil sands magazine, 2018)**

### 1.3.1 Extraction

For extraction, the common way is to mix crushed ores with hot water and caustic soda, known as originally Clark Hot Water Extraction (CHWE) (Masliyah et al, 2004). Solids and bitumen are separated because of the significant difference in wettability of those two components during the liberation process. Large sand grains fall down to bottom due to their high density and most of bituminous components is liberated and suspended in the middle slurry.

The other key part of extraction is bitumen aeration. Air bubbles are generated either in hydro-transportation or floatation cells and small bitumen droplets in water can attach on bubbles thus float to the upper layer for further froth treatment.

The two processes require conflicting aqueous environment. From a scientific view, higher pH leads to ionization of silica surface that becomes more hydrophilic with more negative surface potential, helping the separation of minerals and negatively charged bitumen. Natural surfactants are released from bitumen to aqueous phase because of their ionization of high pH. The surface

tensions between solid and water and between bitumen and water are further lowered (Basu et al, 1997). As for aeration process, it requires a lower pH environment for increasing the interfacial tensions of air-water and bitumen-water system. High pH makes it difficult for highly negative bitumen drops attaching to air bubbles. Because liberation and aeration are conducted in the same aqueous phase, industrial applications optimize the pH contradiction by controlling pH between 8 ~ 8.5.

For mineral solids in extraction process, poor processing ores contain higher percentage of fines which are also more hydrophobic as compared with that of good processing ores, meaning that the fines are more likely to attach to bitumen due to the hydrophobic nature and hinder the coagulation of bitumen drops and attachment to the air bubbles, especially in process water of high calcium concentrations where the electrostatic repulsion of fines and bitumen is mostly screened, resulting in the slime coating (Liu et al, 2004). Researchers also showed that among various types of clays, montmorillonite (less than 1%) attached strongly on bitumen surface in the presence of calcium, as compared with weak attachment of kaolinite (Liu et al, 2004). As a result both percentage and types of fines and clays may influence adversely on extraction process.

### 1.3.2 Froth Treatment

Froth collected from extraction contains typically 60% bitumen, 30% water and 10% solids on mass (Masliyah, 2012). Further dehydration takes advantage of gravity separation by adding light organic diluents to the system. The organic phase of diluted bitumen with lower density and viscosity leads to phase separation. Based on the types of hydrocarbon in organic diluents, the process is classified to naphthenic and paraffinic froth treatment (NFT and PFT).

PFT achieves lower water and solid percentage but lower yield (Shelfantook, 2004; Romanova et al, 2004) due to precipitation of asphaltenes, a critical bituminous component (18%) which is less soluble in paraffinic diluent. The heavy fraction of asphaltenes (50%) (Oil Sands Magazine, 2018) is precipitated out and settle down with water and solids entrapped inside bitumen. The high quality product of PFT can be easily transported long distance to refinery without further upgrading. Naphthenic process is also commercially used because of low cost, high yield and different operation procedures based on product quality required.

Remaining water in bitumen product is inside stable emulsions (<10μm), causing further issues such as higher viscosity, pipeline corrosion, catalyst poisoning and high-coking propensity (Rao et al, 2013). Researchers find that asphaltenes concentration plays a critical role in emulsion stability by forming a solid-like film surrounding the water droplet (Kuamr et al, 2001; Rondon et al, 2008; Harbottle et al, 2014). To destabilize these emulsions, hydrophilic demulsifiers such as ethylcellulose (Pensini et al, 2014) and ethylene oxide-propylene oxide (EO-PO) copolymers (Fend et al, 2010) are applied to compete with hydrophobic natural surfactants at the oil-water interface. The rigid film is penetrated and softened to liquid-like state, eventually leading to coalescence.

Similar to extraction, fine particles is also a detrimental factor here. They are adsorbed on ashpaltenes and resins along with natural surfactants for forming the rigid layer stabilizing water-in-oil emulsions (<10μm). It was found that high pH of the system increases the negative charges of kaolinite surface and decreases the absorption of naphthenates, making it more water-wet and thus less stable emulsions (Jiang et al, 2011). In addition, totally removal of solids achieves completely separation of water and oil without the formation of rug layers (Jiang et al, 2009). Components of organic phase also change the stability of emulsions by depositing natural

surfactants from minerals surfaces, creating weaker interactions due to polarity (Chen et al, 1999) or reducing the density and viscosity of the system (Jiang et al, 2009).

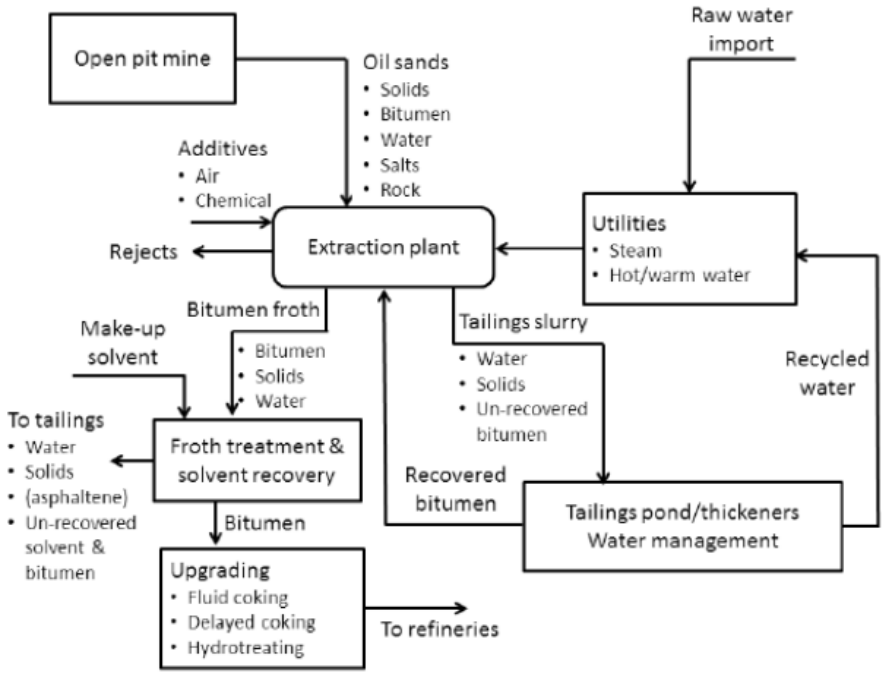


**Figure 1.5 Hot water extraction process (Masliyah et al, 2012)**

## 1.4 Oil Sands Tailings

### 1.4.1 Tailings Ponds

The underflow from extraction and froth treatment facility containing process-attended water, solids and residual organic matter is disposed to tailings ponds which cover as large as 130km$^2$ up to 2011 (Masliyah, 2012). Then it is reported to cover 220km$^2$ by 2017 (McNeill, 2017). The total volume keeps increasing in a current speed at 74 million m$^3$/year (Oil Sands Magazine, 2018) and is a certain threat to the local ecosystem and human safety (NRDC, 2017). Directive 074 and 085 proposed by Alberta Energy Regulator in recent 10 years are aimed to force the industry to reduce the tailings volume and reclaim the land (AER, 2009; AER, 2017). However, it is estimated from

the industry's committed plans that we still need to wait 20 years before the tailings ponds stop expanding (McNeill, 2017). Apparently new technologies are urged for faster tailings settling, more consolidated solids structure, less residual hydrocarbons and more water recycled in shorter time (Matthews, 2011).

### 1.4.2 Composition of Oil Sands Tailings

Tailings coming from the underflow of extraction or froth treatment contain mainly water and mineral solids with weight percent from 0.5% to 10%. There is also a small amount of residual bitumen (1%-3%) and high concentrations of salts.

Among the solids, the coarse tailings defined as solid particles bigger than 44μm contains 55-75% of the original oil sands deposit (Oil Sands Magazine, 2018). They can be classified if the tailings streams are processed by a hydrocyclone. The underflow can settle rapidly and gain enough strength for construction use such as tailings ponds dykes. On the other hand, particles smaller than 44μm defined as fines coming from either hydrocyclone overflow or beaching deposition run-off. Those containing 10-30% of oil sands deposit settle in a rather low rate. Settling from originally 0.5% solids to 30% solids may take up to several months. Without further densification technologies, those which are defined as fluid fine tailings (FFT) or mature fine tailings (MFT) can remain in tailings ponds unsettled for up to 150 years.

### 1.4.3 Thickening Process

Recent years, instead of depositing tailings directly to the tailings ponds, thickeners are introduced to oil sands industry, aiming to get quicker settlement and hot water recycle (Figure 1.6).

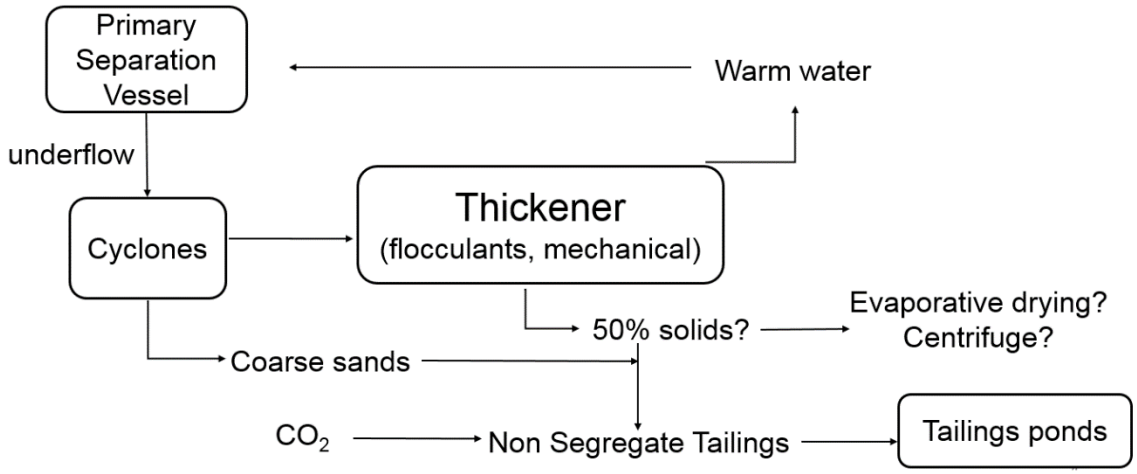


**Figure 1.6 Process of tailings thickening**

Firstly the underflow of PSV is transported into cyclones for classification. The overflow from cyclones is further directed to the thickener where industry uses chemical and mechanical forces to achieve a faster settlement than in tailings ponds. The upper material from the thickener is water to be recycled back to PSV, which remains at a high temperature. The underflows of thickeners is aimed to be 50% solids which can be mixed up with coarse sands and $CO_2$ to form non segregate tailings.

For thickening process, two main chemicals are widely applied in the whole mineral processing industry: the addition of inorganic salts to destabilize fine particles to form aggregates by decreasing surface potentials via particle surface adsorption and screening electrostatic repulsions between particles; the addition of polymeric materials to bridge the fine particles via hydrogen bound or electro static attraction to form large flocs. The effectiveness of these two methods relies deeply on the process water chemistry, the electrostatic property of particles and chemistry/physical properties of the added chemicals. In the oil sands industry, either of these two techniques is applied for faster settling of the fine tailings particles before further densification

using external energies such as evaporating, centrifugation, filtration, freeze-thaw and biogenic process (Wang et al, 2014; Guo, 2009). From the observation of this research, flocculation can always form a stronger and larger structure of aggregates than coagulation, likely due to the stronger chain structures of polymers.

## 1.5 In-situ Recovery

In 1970s, Dr. Roger Butler and his team first developed the steam-assisted gravity drainage (SAGD) method from cyclic steam stimulation (CSS) method originally used for heavy oil production in California. Both of methods rely on the steam injection delivering heat into deep ground to reduce the viscosity of the crude oil or bitumen (McLennan et al, 2005). SAGD enhances the transportation of heat by sending stream down through upper pipes passing horizontally through the formation and collecting the heated bitumen with a lower pipe (Figure 1.7).

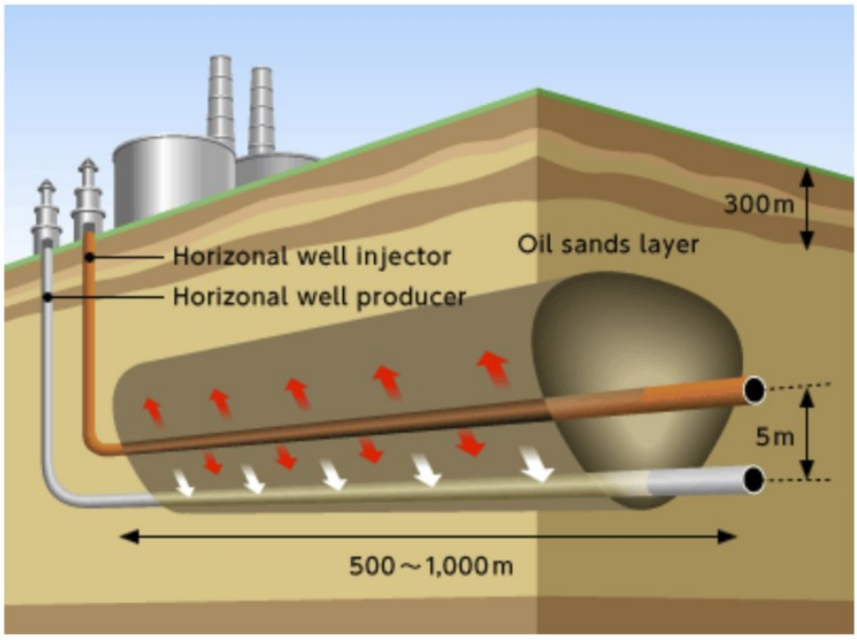


**Figure 1.7 Graphic description of steam-assisted gravity drainage (JAPEX, 2017)**

This technology produces negligible by-products such as tailings although with disadvantages of more water and natural gas usage. It has been grown rapidly to large production of crude oil in recent 30 years (Figure 1.4).

## 1.6 Objectives and Organization of Thesis

The objective of this thesis is to use a combination of inorganic coagulants (calcium oxide/lime) and different types of polymeric flocculants with opposite charge properties to achieve an improved performance of oil sands tailings settlement with higher initial settling rate, lower turbidity of supernatant and higher consolidation of solid sediments. We explain the treatment mechanisms through analysis of electrostatic interactions and interfacial adsorptions of polymers using various experimental techniques such as zeta phoremeter and quartz crystal microbalance with dissipation (QCMD). The organization of thesis chapters is as follows:

Chapter 1 provides an industrial background relevant to the research, including open pit mining and in situ bitumen recovery, along with main procedures of oil sands tailings treatment.

Chapter 2 provides literature review on surface chemistry, colloidal science of oil sands tailings particles, researched polymers as oil sands tailings flocculants and adsorption mechanisms of polymers on particle surfaces.

Chapter 3 describes the design of the experiments, important procedures regarding to measurements and theoretical principles of various instruments used in this research.

Chapter 4 reports the results of fundamental oil sands tailings settlement experiments. Results of ISR, turbidity, consolidation and pH of the system are reported. Results of FBRM monitoring on particle size changes during the flocculation process are also reported.

Chapter 5 shows the utilization of zeta potential measurement and QCMD experiments to explain the optimized performance by the addition of lime, detecting zeta potentials changes of mineral surfaces, enhanced adsorptions of polymeric materials and configuration changes.

Chapter 6 presents conclusions of the research.

# Chapter 2 Theoretical Background and Literature Review

In this chapter, we will review basic knowledges regarding colloidal stability, interactions between charged interfaces and electric double layers based on which we can explain the influence of water chemistry we modify in the tailings system on settling performance. We will also cover recent research of oil sands flocculation process by using polymers with different charges and structures. At last, we will review more on the polymer adsorption on charged surfaces, which helps us explain the mechanism of adsorption and flocculation improvements we see in our experiments.

## 2.1 Electric Double Layer

### 2.1.1 Origin of Electric Double Layer

The origin of electric double layer (EDL) is the charged particles surface. Particles in aqueous environment are usually charged by various causes (Berg, 2010): 1. Preferential adsorption of one type of ions on the interface occurs on crystalline species such as silver halides (AgI) when it partially dissolves and $Ag^+$ tends to desorb quicker, thus excess of $I^-$ negatively charges the surface (Hiemstra, 2012); 2. Ionization of functional groups on particle surface by water chemistry such as hydroxyl groups on mineral surface and protonation/deprotonation of amino and carboxyl groups in proteins protonated/deprotonated by changing pH (Wieland et al, 1992; Salgin et al, 2012); 3. Isomorphic substitution of higher valent ions by lower valent ions in crystalline mineral surfaces (Ma et al, 1999); and 4. Adsorption of charged species such as surfactants and flocculants.

### 2.1.2 Models for Electric Double Layer and Definition of Zeta Potentials

These possibilities can all lead to a charged particle surface which further causes the electric field surrounding the particles in aqueous media. In this field, oppositely charged ions from the system are concentrated to and the same charged ions are repelled from the charged surfaces. Stern model

(Berg, 2010; Masliyah et al, 2006) combining with Helmholtz model and Gouy-Chapman model purposed two main layers of imbalance of charges in the media: first, a number of oppositely charged ions are attracted and adsorbed on the charged interface and immobilized, the plane where the centers of the immobilized ions located is defined as Stern Plane, the space from Stern Plane to the further point where there is no slipping of ions to the surface (Shear Plane) is defined as Stern layer; The space from this point to the bulk solution is defined as Diffuse Layer where the transport and distribution of ions are determined by the balance of electrostatic attraction and diffusion. Later Grahame (Grahame, 1947) and Bockris, Devanathan and Müller (Bockris et al, 1963) modified the model where solvent molecules attached to the interface are taken into account and partially solvated ions are adsorbed on the solvated ion layer. Stern plane is replaced by inner Helmholtz plane which passes through the centers of solvent molecules and outer Helmholtz plane which passes through the centers of adsorbed ions. The BDM model is most commonly used at this moment.

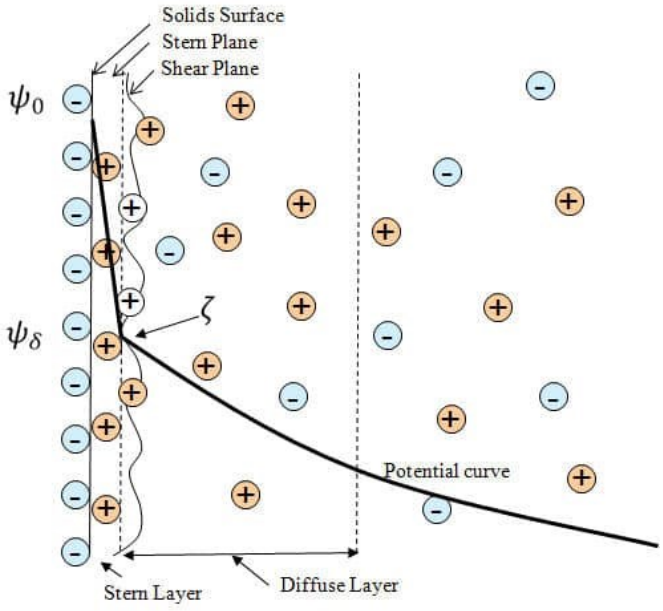


**Figure 2.1 Electric double layer according to Stern's model (Yoon, 2016)**

Here we adapt the simpler Stern model to understand the electrostatic interactions between particles and the concept of zeta potential. The potential decreases from the surface of the particle linearly in Stern layer because of the immobilized counter-ions. The potential on the Stern Plane is defined as the Stern potential which can be measured by fitting the quantitative relationship of potentials (measured by Atomic Force Microscopy) and the distance to Stern Plane based on DLVO theory (Yan et al, 2013). Out of Stern Plane the potential decreases exponentially. The potential on the Shear Plane is defined as zeta potential which can be determined by measuring the electrokinetic behaviors (Hunter, 1981) and electroacoustic behaviors of the particles (Dukhin et al, 2002). Zeta potential is the main factor influencing the dynamics of the particle system. For oil sands fines, the zeta potential is negative and high in the process water (Liu et al, 2004), thus leading to strong repulsion between particles and stabilizes the system.

## 2.2 DLVO theory

Between the molecules and atoms, there is a weak short-distance force caused by induced dipoles in the electron clouds of both atoms/molecules, an induced dipole in one and permanent dipole in the other or permanent dipoles of both (Berg, 2010). This is defined as van der Waals forces which are repulsive if the atoms are too close because of the contact of electron clouds, but are attractive in longer range beyond the van der Waals contact distance (Figure 2.2). The combination of van der Waals force and electrostatic force induced by the electric double layer of particles dominates other forces to determine the stability of the suspension system. Derjaguin and Landau (Derjaguin et al, 1941) and Verwey and Overbeek (Verwey, 1948) separately proposed theories on the same subject in 1940s and this is commonly recognized as DLVO theory.

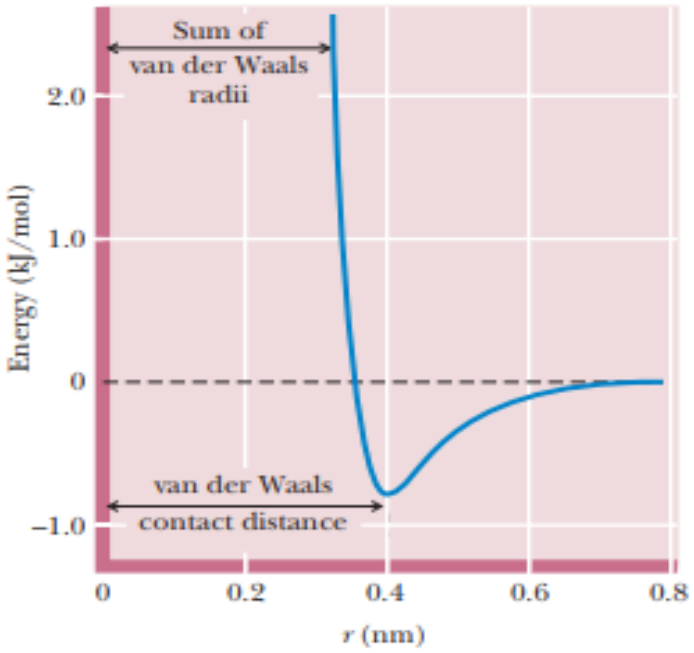


**Figure 2.2 Energy profile of van der Waals forces vs. distance between atoms (Garrett et al, 2010)**

For a common system such as oil sands tailings, most particles in process water have negative zeta potentials, meaning that they are negatively charged (Liu et al, 2004). Thus the electrostatic force and van der Waals force are two opposite interactions, both decreasing as the distance increases. But the electrostatic force has a dominant influence in intermediate range and can be feasibly affected by water chemistry. As Figure 2.3 demonstrates, as the surfaces of two particles get closer, the energy would first enter a trap where both of the forces are weak and van der Waals forces overpowers, termed as secondary minimum. The energy of this trap can be easily overcome by thermal stimulation and external perturbation. As a result, the stability of the particle system can become tuned reversibly. As the distance decreases, the particles would experience an energy barrier where EDL repulsions dominate (Boström et al, 2006). This energy barrier formed by EDL repulsions can prevent particles from aggregation. As the concentration of electrolytes increases,

the repulsion can be screened. When the barrier is low enough the thermal energy of particles can overcome the barrier. Then the particles reach the primary minimum, binding by short ranged van der Waals forces to form the aggregates. This binding is irreversible.

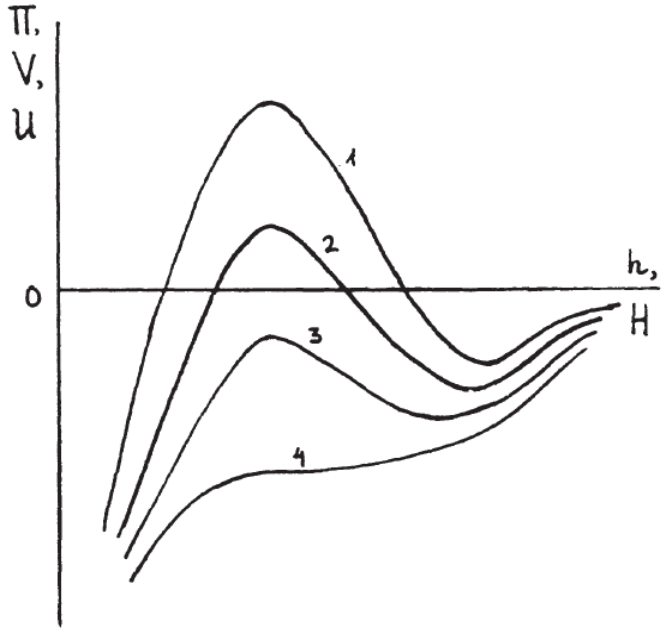


**Figure 2.3 Interaction energy between particles based on DLVO theory. Electrolyte concentrations increases from 1-4 (Derjaguin et al, 1987)**

## 2.3 Compositions and Mineral Structure of MFT

The fine particles of MFT settle down to around 30% solids and become stabilized by strong electrostatic repulsions. Such behavior results from the unique compositions and structures of minerals in oil sands. Typical oil sands fine solids contain kaolinite (69%), illite (28%) and smectite (under 1%) (Cuddy, 2004). Kaolinite is a two-layer clay with one tetrahedral silicon oxide layer and one octahedral aluminum hydroxide layer (Figure 2.4). The two layers are connected by hydrogen bonds between the hydroxyl groups in aluminous layers and the oxygens in siliceous layer (Konan et al, 2007). Each basal layers and the edge layer have distinct surface electric

characteristics with changing aqueous pH. The pH-insensitive charge on both types of basal surfaces results from the cation isomorphic substitutions, while the pH-sensitive charges result from the hydrolysis reactions of Al-OH basal surface and broken Al-O/Si-O bonds on edge surface (Masliyah, 2011).

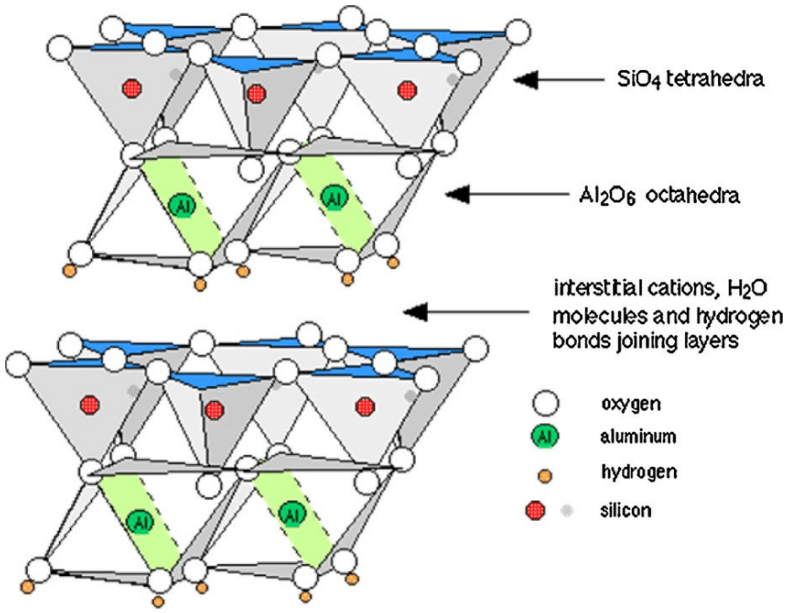


**Figure 2.4 Structure of kaolinite (Valapa et al, 2017)**

Zeta potentials of kaolinite vary from positive in low pH to negative in high pH. In varying pH, the aluminous and siliceous basal surfaces and the edge surface may carry different amounts or types of charges (Yan, 2013), leading to yield strength and structure changes such as card-house structure (Figure 2.5). Similar characteristics of surface charges are observed on illite (Long et al, 2006) which has a three-layer structure with one aluminous layer sandwiched by two siliceous layers, thus acquiring more negative charges than kaolinite. The high calcium adsorption capacity and swelling effect of Montmorillonite (Liu et al, 2004) result in its devastating role in extraction and tailings treatment process despite its small amount of less than 1%.

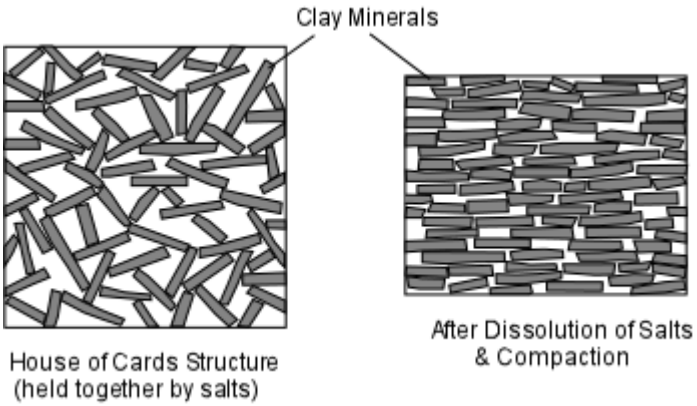


**Figure 2.5 Card-House structure of plate minerals (Nelson, 2015)**

## 2.4 Coagulation and Flocculation

In order to collect fine particles in oil sands and other mineral industries, the energy barriers between each pair of particles have to be either overwhelmed by external attractive forces or be suppressed to be lower than other attractions, such as bridging forces or thermal motion energies. The first method can be achieved by using mechanical forces such as centrifuge (Rao et al, 2015) and filtration (Alamgir et al, 2012) though centrifuge is considered as cost inefficient because of high speed movement, while filtration needs to be associated with flocculants-aid to achieve high solid content. A novel technology involving mechanical screw press is introduced to oil sands tailings treatment recently and results in a drastic improvement for dewatering efficiency and product strength (Wang, 2017).

Using chemical additions such as high molecular weight polymers as flocculants provides an economical way to achieve fast settling by gravity and high solid content in sediments. This involves bridging mechanism which was first defined by Ruehrwein et al in 1952. The chain of polymer connects several particles via either electrostatic attraction or non-electrostatic force such as hydrogen bonds (Figure 2.6-a, c). In this system, the energy barriers between particles become

less important due to the bridge of particles at relatively large distances by polymer chains. As a result, larger flocs are formed for them to settle out rapidly. An optimum dosage of polymers is observed and the flocculation behavior decays after this dosage (Gregory, 1988). The possible explanation is excessive polymer chains cover the surface of the individual particles and make them hardly to be bridged by other polymer chains. The optimum dosage is purposed as the dosage where half of surface area is covered by polymers.

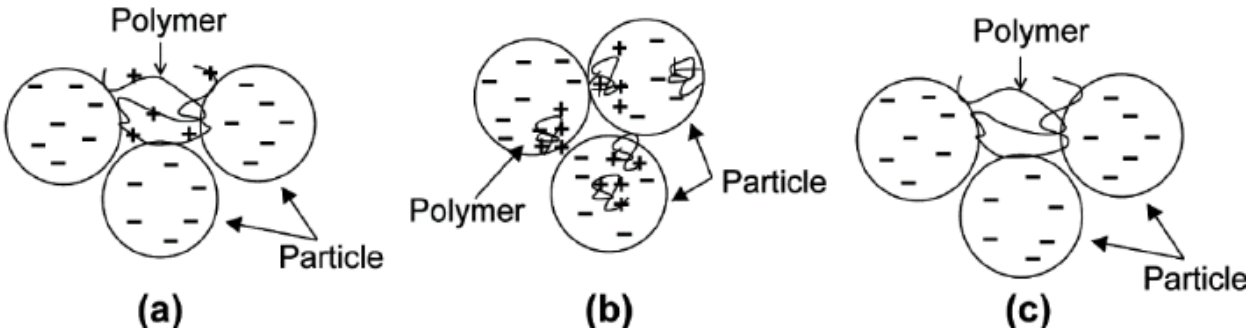


**Figure 2.6 Roles of polymers in fine particle flocculation (Dobias et al, 2005)**

Other than bridging effect based on the polymer configurations in suspensions, there is also patching behavior of oppositely charged low molecular weight polymers on the particle surface based on strong electrostatic attractions and less steric hindrance (Gregory, 1972) (Figure 2.6-b). This can improve the flocculation rate if the overall surface potentials of particles are close to zero, similar to coagulation mechanism which we will discuss later. The difference from coagulation using inorganic ions is that the short polymer chains attached on multiple particles may result in a much stronger structure of the floc as compared with coagulation. A great performance is observed with dual polymer addition into MFT involving a type of short chain cationic polymer and a type

of relatively long chain anionic polymer (Wang, 2017). The short chain cationic polymer patch is possibly the key part for increasing the strength of the flocs.

Using inorganic salts as coagulants to gather fine particles in water industries has been a great success (Jiang, 2015). It is termed as particles agglomeration and precipitation via the electric double layer compression, usually by inorganic salts. The electrostatic repulsive forces are suppressed because of increasing ion strength. Based on DLVO theory the van der Waals forces overcomes electrostatic repulsion in short ranges (Figure 2.3) and the particle system can easily reach the primary minimum by thermal perturbation. For multi valent ions such as $Ca^{2+}$ and $Al^{3+}$, hydrolyzed ions composed of the metal ion and hydroxide ions are considered likely to attach to the mineral surface with OH or O group via hydrogen bonds (James et al, 1972). If those hydrolyzed ions still carry positive charges ($CaOH^{+}$, $Al(OH)_2^{+}$, etc.), the surface potential of negatively charged particles such as kaolinite can be reversed at corresponding pH (Mpofu et al, 2003). This can also result in more effective system destabilization, leading to coagulation which may influence polyelectrolyte adsorption in further flocculation process. In water treatment process, due to the low solid content and fine size of suspended particles, excessive amount of multivalent ions are more likely to form precipitates or hydroxide complexes surrounding smaller solid particles to capture or entrap them inside to settle down, which is termed as “sweep effect”. Another important mechanism is forming the precipitates on the larger particle surfaces by metal ions in relatively high pH. For example, the hydroxide or carbonate precipitates formed may have a higher point of zero charge than mineral particle surfaces in the same water chemistry, resulting in a positive surface potential of the covered particle (Atesok et al, 1988).

For oil sands tailings treatment, small amount of calcium (gypsum) is added into tailings ponds order to enhance the settling of fluid fine tailings. Comparing with flocculation, this has low

efficiency, as it only forms small aggregates of weak structures, which limits the sole usage of inorganic salts for further improvement. Although calcium is the key factor for clarifying upper layer water, the recycle water is required to contain low calcium ions for extraction process as discussed in the previous chapter.

## 2.5 Polymers for Oil Sands Tailings Treatment

Various polymers have been applied for flocculation of oil sands tailings in industrial applications or research. Polyacrylamide (PAM) based polymers are most commonly used and studied. It is considered that free hydroxyl groups from AlOH or SiOH on the basal or edge surface of kaolinite can form hydrogen bonds with the oxygens of acryl groups (Nabzar et al, 1984). In addition to these bonds there are also electrostatic attractions/repulsions if PAM chains are chemically modified with charged groups (Figure 2.7). Hydrolyzed PAM (HPAM) is one of negatively charged PAM by either partially hydrolyzing in weak basic aqueous or copolymerization with acrylic acid. Although the negative charge feature repulses the tailings particle surfaces and reduces the polymer adsorption (Wang et al, 2014), there still exists a significant amount of adsorption and efficient performance of settling because compared with nonionic PAM, the charged groups of HPAM can extend the chain and enlarge the conformation of the polymer coil by repulsions, which benefits the bridging effects. On the other hand, cationic polymers can be obtained by copolymerization with monomers of quaternary ammonium groups such as diallyl dimethylammonium chloride (DADMAC). Cationic polymers gain a large amount of adsorption on negatively charged minerals, which also leads to a flatter adsorption layer on the particle surface. The mechanism of flocculation by cationic PAM is more likely dominated by electrostatic patch and charge neutralization. These require a higher dosage of cationic polymer than anionic PAM with similar molecular weight as observed in this thesis and previous studies (Wang, 2017).

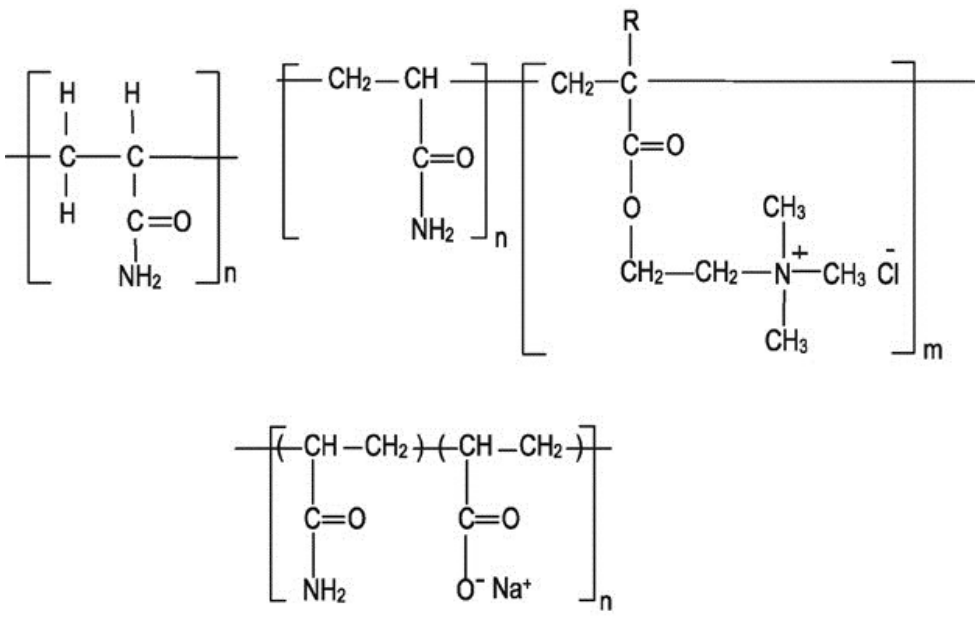

**Figure 2.7 Nonionic, cationic and anionic polyacrylamide (Vedoy et al, 2015)**

Other than charged PAM which can be acquired commercially and applied in large scales, researchers have been synthesizing novel polymers with sensitive features or unique structures to gain flocculation improvements. The structure of N-isopropylacrylamide (NIPAM) contains both hydrophobic parts (ethylene backbones and isopropyl groups) and hydrophilic parts (carbonyl groups of acrylamide) in room temperature. Once above the 32 $^{o}$C which is termed as lower critical solution temperature, the hydrogen bonds between water and the hydrophilic parts are no longer stable and are prevailed by intramolecular hydrogen bonds. Thus the polymers tend to be hydrophobic and settle out. By copolymerization with PAM this temperature sensitive behavior has been applied to oil sands tailings (Li et al, 2007; Chan, 2011) After temperature sensitive polymers are mixed with diluted tailings particles at room temperature to form loose structure flocs, the temperature is increased to contract the structure to form more compacted flocs (Figure 2.8), achieving high efficiency of dewatering.

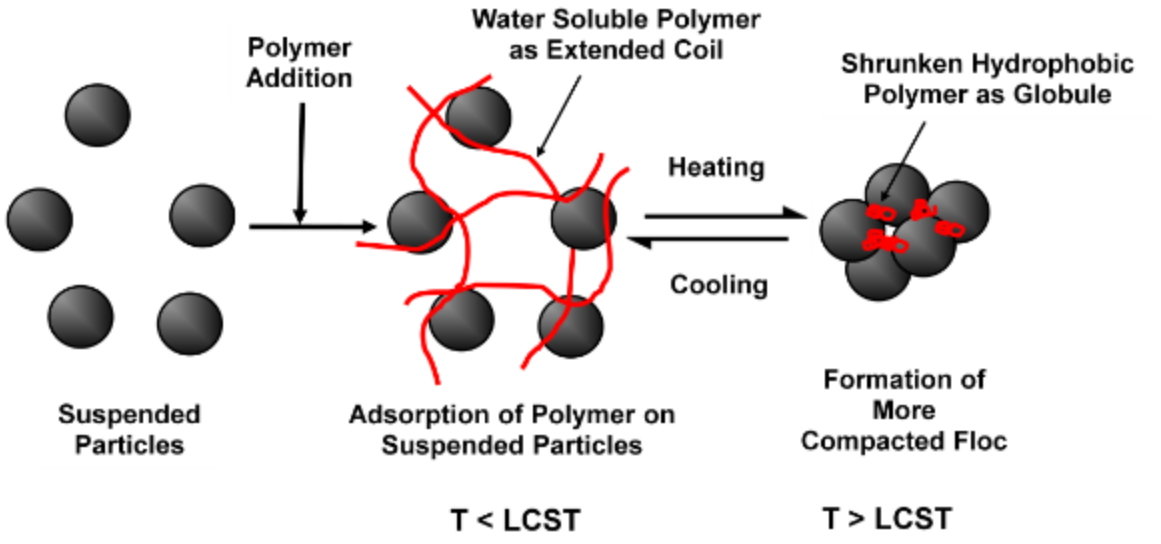


**Figure 2.8 Temperature sensitive polymer flocculation mechanism (Li et al, 2006)**

The pH sensitive polymers basically have the same hydrophilic-hydrophobic transition feature responding to the change of aqueous pH. The mechanism relies on the pH responsive groups connecting to the ethylene backbone, such as the tertiary amine groups from DMAEMA (2-dimethylamino ethyl methacrylate) and carboxyl groups from acrylate. The groups can be either protonated or deprotonated by changing pH. By designing the ratio of the monomers with pH responsive groups and pure acrylamide monomers (Guo, 2015), a pH sensitive polymer can be hydrophilic at relatively high and low pH, and be hydrophobic in the intermediate range of pH, because positive pronated tertiary amine and negative carboxyl exist at the same time forming so called zwitterionic polymers. The whole individual polymer chain is contracted by intramolecular attractions of the two counter ionic groups. In the pH of process water, hydrophilic zwitterionic polymers are adsorbed by tailings particles via hydrogen bonds from acrylamide segments. Then the system is properly acidified, leading to more water to be drained from compacted flocs.

Besides of using external stimuli to change the configurations of polymeric flocculants, hybrid polymers are also studied. It involves grafting organic polymers onto inorganic particles as the cores. $Al(OH)_3$-polyacrylamide (AlPAM) is first created by Yang et al in 2004. By using $Al(OH)_3$ nanoparticles adsorbing persulfate initiators, the polymerization of PAM initiates from the surface of $Al(OH)_3$ to form star-like or network-like structure.

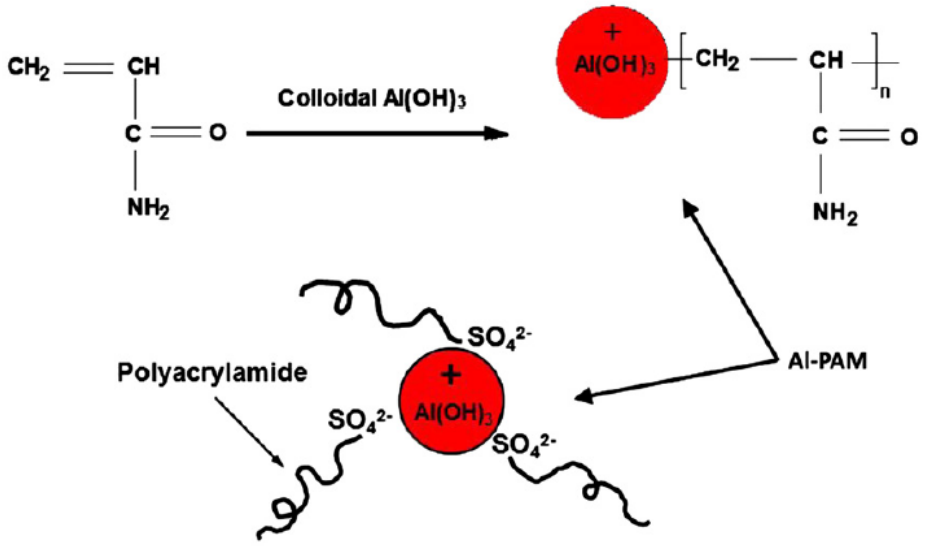


**Figure 2.9 AlPAM star-like structures (Alamgir et al, 2012)**

The positively charged cores tend to attract more negative tailings particles. The network-like or star-like structure provides a much higher strength to bridge the particles. Such binding structure results in more dense flocs. The drawback of this type of polymers is that most of the PAM chains are connected (concentrated) around the cores. The larger structure thus is not as diffusive as individual PAM chains. It requires a high dosage to form settlement, close to that of cationic polymers.

Other hybrid polymers such as $Fe(OH)_3$-PAM, Chitosan-g-polyacrylamide and sodium alginate-g-PAM are also created and applied to mineral tailings treatment, showing better performance (Wang et al, 2014; Wang et al, 2015; Tripathy et al, 1999).

## 2.6 Adsorption of Polymers on Mineral Surfaces

In aqueous environment with soluble polymers, the mineral surface can adsorb polymers via electrostatic forces in long ranges or non-electrostatic forces in short ranges. The adsorption amount depends on the charge density of polymer segments, the surface charge nature of the mineral surface in various pH and also electrolyte concentrations in solvent. As the electrolyte concentrations change, not only the electrostatic attraction/repulsion between polymers and surfaces are screened, also the repulsions between polymer segments are influenced by the higher ionic strength, which results in conformational change of the polymeric flocculants (Roiter et al, 2006). The conformations of polymers adsorbed on the interfaces can be divided into three parts: tails which are the ending segments of polymers mostly in the solution, trains which are the segments mostly attached to the interface and the loops with both ends attached on the interface (Scheutjens et al, 1980).

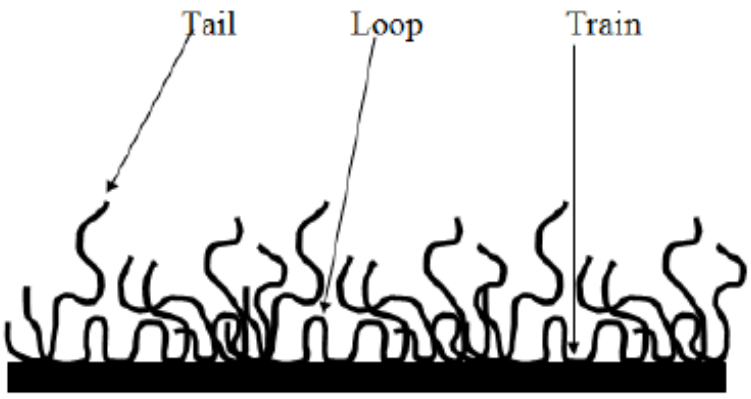


**Figure 2.10 Depiction of loop, tail and train structures of polymer adsorptions (Gurumoorthy et al, 2011)**

The loop and tail structures of polymers contribute to the bridging and flocculation process (Figure 2.10). In high electrolyte concentrations, the adsorbed polyelectrolytes collapse into smaller necklace-like globules (Roiter et al, 2006), eliminating the loop and tail structures and bridging effect.

On the other hand, an extremely extensive conformation of polymer can deteriorate the adsorption process and flocculation as well. According to calculation by Keizer et al., electrolyte concentrations can affect polyelectrolyte adsorption on oppositely charged surface in two opposite ways. For highly charged polymer with non-electrostatic interactions such as hydrogen bonds with the surface, the larger conformations prevent the polymer chains adsorbed densely on the surface due to strong repulsion between charged segments. Thus high salt concentration in this case can screen the repulsion between segments and polymers mainly behave as nonionic polymers which have more loops and tails structures to enhance the adsorption and increase the amount of adsorption. This is called by Keizer the screening – enhanced adsorption regime. On the other hand, for low charged polymer, repulsion between segments is not so strong and high salt concentration can also screen the electrostatic attraction between polymers and the surface, thus polymer adsorption is reduced. Polymers will even desorb if there is no non-electrostatic interaction between polymers and the surface. This is called screening-reduced adsorption regime.

# Chapter 3 Materials, Instruments and Experimental Procedures

## 3.1 Materials

### 3.1.1 Mature Fine Tailings

The mature fine tailings (MFT) used in this research is directly transported from industrial tailings ponds. Because different companies take different procedures for recovery process, the composition of the resulted tailings varies significantly (same as process water). The MFT used in this research came from Canadian Natural Resource Limited (CNRL) sites.

To determine the solid percentage of MFT, a large volume of sample in a pail (diameter 275 mm) is mixed by mechanical impeller (diameter 135 mm) under vigorous speed (~350 rpm) for 30 min, making sure that the whole suspension is uniform and the spooned samples are representative. Four samples about 20 ml each are sent to oven (100 ℃) overnight for dehydration. The average solid content is 29.4%, with standard deviation lower than 0.3%.

### 3.1.2 Process Water

All MFT samples are diluted by process water (PW). For most of the research such as settling tests, FBRM measurements and QCMD measurements, the origin of PW is from the Aurora site of Syncrude. For zeta potential measurement of MFT particles, both Aurora process water and CNRL process water are used for comparison to show the influence of divalent cations in each water.

Following table shows the main ion concentrations in each type of process water (measured by ion chromatography):

**Table 3.1 Main ion concentrations in process water**

| Ion conc. (ppm) | $Na^+$ | $K^+$ | $Mg^{2+}$ | $Ca^{2+}$ | $Cl^-$ | $SO_4^{2-}$ |
|---|---|---|---|---|---|---|
| Aurora | 876 | 15.75 | **12** | **27** | 432 | 333 |
| CNRL | 667 | 16 | **9** | **14** | 498 | 221 |

It can be found that calcium and magnesium ions in APW is much higher while other ion concentrations are basically similar. The significant influence of this difference will be discussed in the further chapter.

3.1.3 Polymers

The polymeric flocculants used are Magnafloc 336 (MF336) and one cationic polymer Zetag 8110 purchased from Ciba Specialty Chemical. Both are white flowing powders sealed in plastic bottles.

Magnafloc 336, with partially hydrolyzed polyacrylamide as the main component, is reported to be a low negative charge density (<10%) polymer with a high molecular weight at around 11.5 million Da. Zetag 8110, with the main component being polyacrylamide derivative with 10% quarternized amine groups, has a 10% permanent positive charge and a molecular weight of 12.7 million Da (Ng, 2018; Wang et al, 2016).

Either polymer with 0.015 g weight is carefully transferred into 50 ml Aurora process water with magnetic stir mixing at vigorous speed overnight to fully dissolve the polymer. The resultant polymer solution is 300 ppm for further dilution if needed. Because pH of APW is around 8.3, this slightly basic environment may lead to polyacrylamide hydrolysis. Also solution ageing may lead to polymer disentanglement or degradation which may change viscosity (Gardner et al, 1979) and

flocculating effectiveness. The polymer solution is always prepared 1 day prior to the experiment and it is regarded as expired once prepared for more than 1 day.

### 3.1.4 Calcium Oxide (Lime)

Calcium oxide is purchased from Sigma-Aldrich (product No. 208159 ALDRICH, ReagentPlus®, 99.9% trace metals basis). The material is a white fine powder reacting with $CO_2$ and $H_2O$ in air. According to the vendor's description, extra 10% of the stated mass is given to compensate for the loss of reactions with $CO_2$ in air. The product container is well sealed with parafilm after received. During the project a sample was taken to test in thermal gravimetric analysis (TGA), and the results are compared with that of pure calcium hydroxide and pure calcium carbonate. The $H_2O$ and $CO_2$ are released during thermal decomposition in the rising temperature of TGA, at 320 ~ 500 ºC and 600 ~ 820 ºC, respectively (Figure 3.1, Figure 3.2). According to the weight loss of calcium oxide in those temperature ranges, the compositions are calculated, showing 80.1% $Ca(OH)_2$ and 16.5% $CaCO_3$ (Figure 3.3).

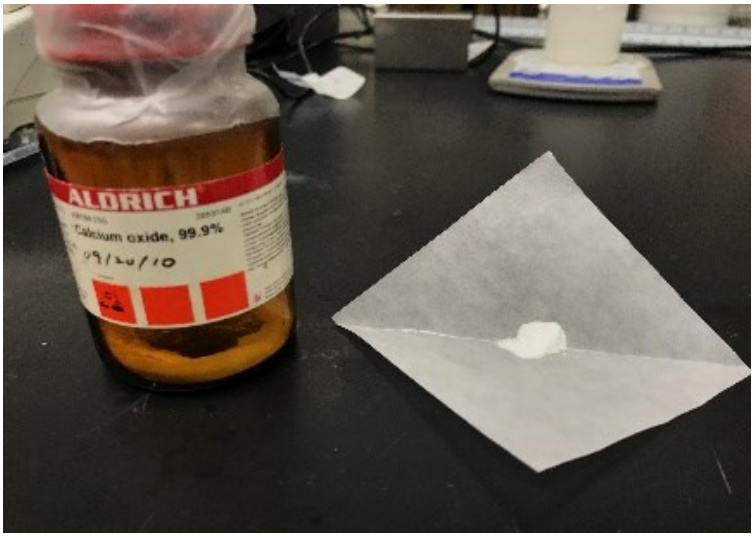


**Figure 3.1 Lime used in experiments**

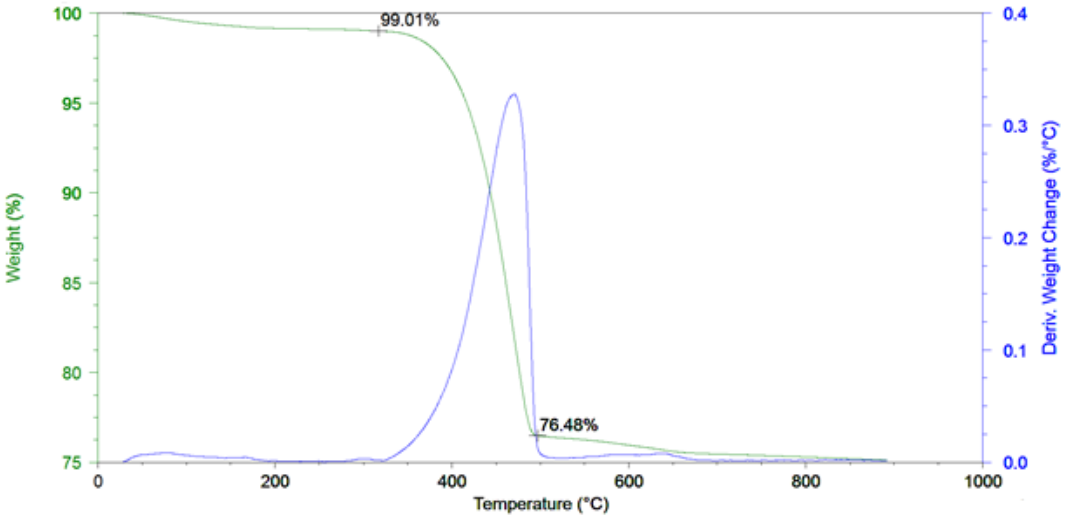


**Figure 3.2 TGA result of pure calcium hydroxide**

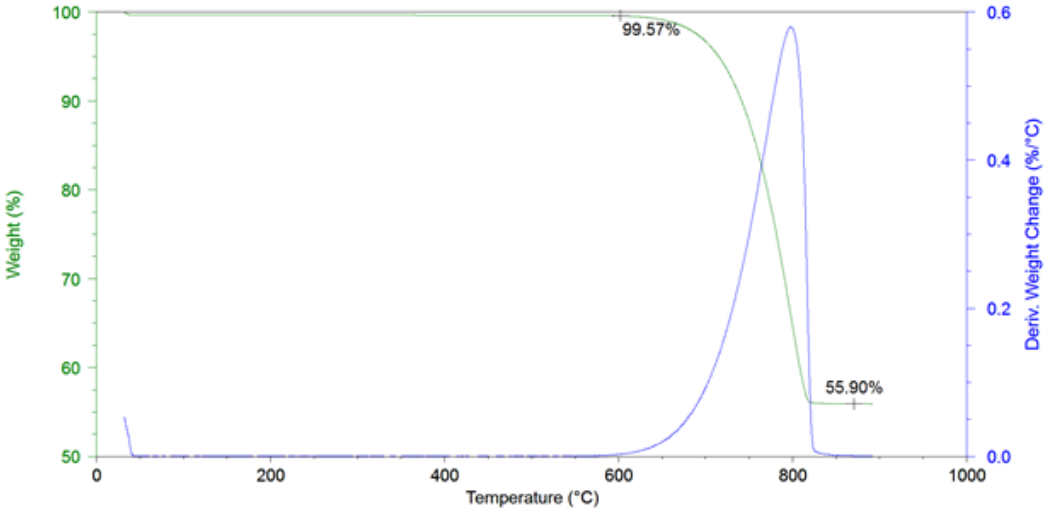


**Figure 3.3 TGA result of pure calcium carbonate**

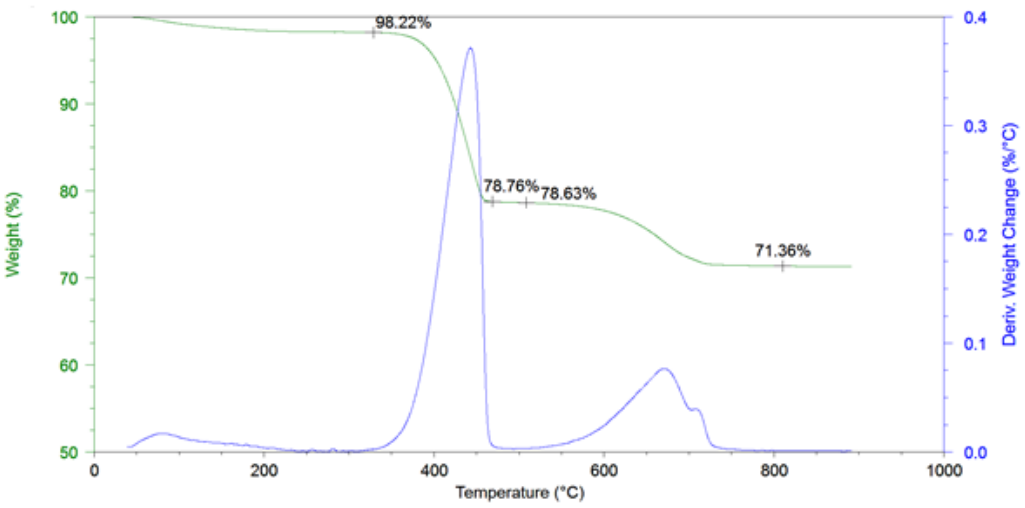


**Figure 3.4 TGA result of purchased calcium oxide**

## 3.2 Instruments and Procedures

### 3.2.1 Cylinder Settling Tests

A proper amount of fresh lime is weighed and added into Aurora process water, mixed by magnetic stirrer for 2 h (Figure 3.5-a). Then the system is settled by gravity for 0.5 h before the clear upper layer is formed (Figure 3.5-b). Plastic pipettes are used to transport the supernatant into the 100 mL cylinder on the balance. Around 3.4 g of CNRL MFT is added to the total solid content added around 1 g. Then a pre-diluted polymer solution (Magnafloc 336 or Zetag 8110) is added to a total system volume of 100 mL. Different concentrations of polymers and lime are tested for settling tests. The final concentration of anionic polymer Magnafloc336 is ranged from 2 ppm to 4 ppm of suspension. The concentration of lime which means the amount of lime used in the mixing procedure divided by the volume of settling tests is from 7.5 mmol/L to 30 mmol/L. The solid percentage of tailings solid in the cylinder is 1%.


**Figure 3.5a Lime suspension (15 mM) after 2h mixing**


**Figure 3.5b Lime suspension (15 mM) after 0.5h settling**

After all chemicals are added the cylinder is sealed by parafilm and inversed vertically 5 times for uniform mixing of tailings, lime and polymers. Then the cylinder is set on the horizontal table and the mudline height of the tailings is immediately recorded as a function of time (Figure 3.6). The mudline dropping rate is decreased with time, which reveals a negatively exponential feature. The initial settling rate which is the slope of the mudline height change at time 0 is estimated by linearly fitting the first few records of mudline height at the beginning. For low dosages of lime there might be a second mudline which would not be recorded in initial settling rate tests as the second mud layer formed contains a very low amount of solid.

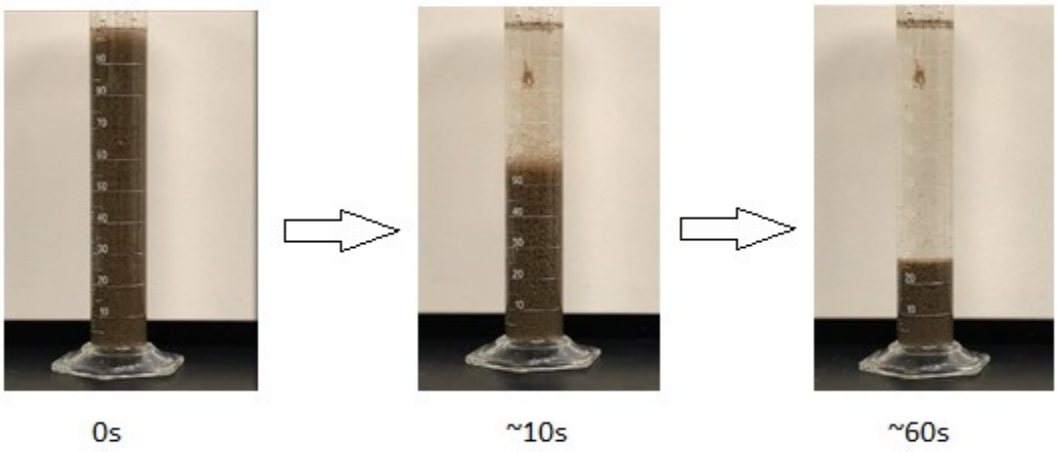


**Figure 3.6 Settling tests with 15mM lime and 3 ppm MF336**

3.2.2 Focused Beam Reflectance Measurement

Focused beam reflectance measurement can determine size distributions of the particle system in situ and in real time during the aggregation and flocculation process. As the sample flows by the probe, a laser beam is focused through the probe tube to the sample particles. The optics emitting the beam rotates at a high speed thus the beam can scan over the particles with the reflected beam to be detected. Each pulse of the reflected beam has a distinct duration, which after multiplied by the scan speed represents the individual particle chord length.

The chord length is one basic type of measurement for particle size distribution. The transformation from chord length distribution to particle size distribution is a complex calculation depending on the optic properties and shapes of the particles. Meanwhile, this research uses the mean square weight chord length to represent the size change of the particles during the settling process.

**Procedure**

A 1 wt% MFT sample in 80mL Aurora process water is prepared and mixed in 100 mL beaker of 200 rpm. The probe is inserted into the sample at roughly the middle point of the beaker radius at half of the sample height. After starting the measurement, a proper amount of lime powder is added into the sample. A glass rod is used to help mix to make sure there is no powder residual on the sample surface. The possible coagulation is recorded until measurement becomes stable and a proper amount of polymer solution is injected at a constant rate in 1 min. The floc size is recorded until the measurement becomes stable. The mixing rate is then turned up to 400 rpm for observing the floc breakage under severe agitation.

### 3.2.3 Zeta Phoremeter

Zeta phoremeter is used to measure the zeta potential of MFT particles in process water with different amount of calcium oxide, calcium chloride or at different pH. The weight percentage of solid particles is around 0.1 ~ 0.2% for a proper count of particles by the camera.

The instrument is designed to capture the tracks of particles by a digital camera on an optical microscopy. The suspension is loaded into a transparent and clean quartz cell, the two sides of which are under a constant electric field. The charged particles start to move in a specific direction and average velocity. The microscopy is carefully adjusted to allow the camera to capture the motions of particles in the stationary layer where the particle motions are not influenced by the electro-osmosis effect because of the charged quartz cell wall (Hunter et al, 1981). Based on the motions captured the average electrophoresis velocity can be calculated. The zeta potential is related to electrophoresis mobility by Smoluchowski:

$$\zeta = \frac{v\eta}{E\varepsilon_r\varepsilon_0}$$

where $\varepsilon_r$ is the dielectric constant of the medium, $\varepsilon_0$ the permittivity of vacuum, $E$ the applied electric field in the cell, $\eta$ the dynamic viscosity of the medium, $v$ the average velocity measured and $\zeta$ the zeta potentials of the particles. This applied to particles of any shape with a thin double layer. In this project all experiments are in aqueous solutions of strong ionic strength because of the process waters. In Aurora PW, the electric double layer calculated based on ions concentration by IC is 1.6 nm. And in CNRL PW, the EDL thickness is 5.5 nm. The average diameter of MFT particles is around 10 micro measured by Malvern Mastersizer.

**Procedure**

The clean quartz cell is put in place with gaskets on both sides between electrodes, inserted on the stage of the microscopy. The 0.01 molar potassium chloride solution is firstly drawn into the cell after each assembly of the cell for calibrating the distance of the electrodes.

After the calibration, the cell is cleaned several times with deionized water before drawing the sample suspension in. The sample is well stirred 5 min before use. For pH adjustment, a proper amount of 1M NaOH drops is added during the mixing, with the pH monitored spontaneously and the sample is immediately drawn in. After checking there is no bubble inside the cell, both stop clocks are closed to seal the cell. To find the stationary layer where the electrophoresis is not influenced by the electro-osmotic effect of the wall, the stage level and laser focus are adjusted constantly till finding the upper wall where the particles are attached to the wall and do not move. Then according to the position calculated by the vendor-provided program, the stage and focus are adjusted to the stationary layer.

Finally, start the program to apply an electric field in the cell and the particle motions are recorded. The distributions of particles mobility and zeta potentials are acquired.

3.2.4 Quartz Crystal Microbalance with Dissipation

The piezoelectric nature of quartz crystal generates mechanical deformation when it is applied with an alternating current. If the electrodes of crystal and the alternating current are properly designed, a resonant oscillation of the crystal can be obtained, the frequency of which is related to the thickness of the materials, thus the deposited mass on the interface. When the alternating current is turned off, the oscillation inside the crystal can in turn generate an oscillating current in the circuit. The resonant frequency and the dissipating factor of the oscillation are quantitatively detected. The Quartz Crystal Microbalance with Dissipation monitoring is aimed to measure the adsorbed mass on quartz sensor which is uniformly coated by a single material representing the surface researched and the layer rigidness based on the dissipation change. The relationship between the resonant frequency shift $\Delta$ and adsorbed mass $m$ per unit area is given by Sauerbrey as (1959):

$$\Delta = -\frac{f^2}{\rho_q v_q} m$$

where $\rho_q$ and $v_q$ are the density and shear wave velocity in quartz, respectively. A trend was observed that a more open and softer layer of adsorbed materials with more bulk liquid yields a larger ratio of dissipation factor shift to frequency shift (Rodahl et al, 1997). A quantitative analysis on the influence of viscoelastic properties of thin layers in Newtonian liquid on the frequency shift and dissipation factor is shown somewhere else (Voinova et al, 1999). Basically a more viscous and less elastic adsorbed layer with larger thickness generates a higher dissipation factor because of the viscous dissipation between the bulk liquid and the layer during the oscillation, though the

frequency shift has no significant difference in liquid as compared with that in vacuum where Sauerbrey's equation applies. This make it possible to assess the adsorbed mass on the surface and the conformation change of polymers in the adsorbed layers by measuring frequency shift and the ratio of dissipation shift to frequency shift using Q-Sense E4. In this research we consider the frequency shift $\Delta F$ as a measurement proportional to the adsorbed polymer mass and the higher ratio of dissipation to frequency shift as indications for less compact adsorbed polymer layers.

**Procedure**

Proir to experiments, the Q-Sense E4 chamber (flow module) which holds one sensor crystal with the measurement liquid flowing beneath during experiments is first immerged in 2% Sodium Dodecyl Sulfate solution (SDS) for 30 min under weak sonication and soaked overnight. Then it is immerged in deionized water for 30 min under weak sonication to wash out the residual chemicals. The tubes transporting liquids by an external peristaltic pump in experiments are cleaned using the same procedure. Nitrogen is used for drying out the chamber and the tubes. The silica coated sensor is placed under UV light for 10 min for decomposing possible residual polymer chains on the surface and then cleaned using the same procedure as cleaning the chamber. After drying, the sensor is placed under UV light for another 10 min.

The sensor is placed in the module and ensured proper contact with the electrodes. The module is assembled into the chamber platform and connected with extremely dry plastic tubes to the air and the external pump on each side. The pump runs at a constant rate of 0.1 ml/min during the experiments. The two pieces of the module is tightly assembled to make sure that the inside is well sealed without liquid leakage.

During the measurement, air is first pumped into get a stable resonant frequency, indicating that there is no residual or humidity on the sensor. Then Aurora process water is pumped in as the bulk liquid. The detection shows drastic change of frequency and dissipation because of the liquid loading on the sensor. The measurement is restarted and the polymer solutions in Aurora process water mixed with lime supernatant of different concentrations is pumped in. The frequency shift and dissipation are recorded until they become constant, followed by pumping the process water are pumped in again to wash away materials weakly adsorbed.

# Chapter 4 Flocculation Performance of Lime Treatment

## 4.1 Cylinder Settling Tests

### 4.1.1 Conditions of Cylinder Settling Tests

In the following experiments, the settling of tailings with various concentrations of polyelectrolytes and lime in cylinders as a model system of fine tailings overflow of oil sands tailings treatment thickener will be reported. The aim of this set of measurements is to investigate the relationships between the initial settling rate measured from descending rate of the first mudline and the concentration of lime. The concentration and the type of flocculants were controlled while varying the concentration of lime. As discussed in Chapter 3, lime is mixed for 2 h and settled for 0.5 h before the supernatant is used. The concentration of lime reported here is calculated by dividing the weight of lime solid added by the weight of process water. It should be noted that the concentrations are expressed in terms of both the weight of undissolved lime and dissolved lime..

The concentration of lime is restricted from 0 mM to 30 mM which is equal to 0 mg/g ~ 168 mg/g on dry solid basis of tailings and equal to 0 ppm ~ 1680 ppm on the basis of whole suspension system (1 wt% solid). For concentration higher than 30 mM , the final pH of settling supernatant is higher than 12 which is unacceptable for recycling use of released water for extractions. In this study five different concentrations of lime distributing evenly in the range were tested. The pH of the system varied from 8.3 to 11.9 as Figure 4.3 shows. In order to measure the performance in pH of around 10.5, extra tests with 10 mM of lime addition to the system were conducted.

With the same concentrations of lime, the concentration of polymers was also changed to confirm the trends observed with varying lime concentrations. The determination of polymer

concentrations was based on the best performance of flocculation with polymer alone. For the anionic polymer Magnafloc336, the best dosage was found to be from 6 ppm to 7 ppm (Figure 4.1). After 7 ppm the ISR decays because of excessive coverage of polymers on the minerals. Therefore 2 ppm and 3 ppm of MF336 concentrations were used in each set of tests. A small number of tests were done in 4 ppm of MF336 as well. The trends of ISR for various polymer concentrations are shown in the following section. For cationic polymer Zetag8110, the ISR was measured without lime addition, and obvious flocs were formed when the dosage of polymers reached 80 ppm on the basis of the suspension system. This observation is consistent with the findings from previous studies (Wang et al, 2016). We used less than half of this dosage when lime addition was involved to investigate the potential of reducing the use of cationic polymers which are more expensive. Zetag8110 concentration of 20 ppm, 30 ppm and 40 ppm was tested separately.

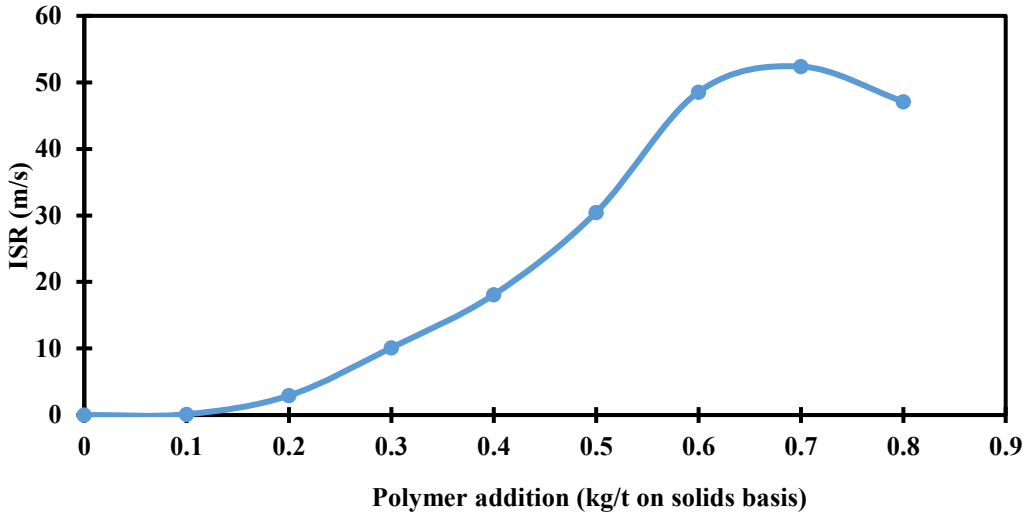


**Figure 4.1 Initial settling rate with MF336 alone in 1% MFT**

To investigate the effect of lime particles on the flocculation, the lime suspension with undissolved particles was used to conduct tests with the same concentrations of MF336. After 2 h

mixing for lime, the settling procedure of lime suspension was skipped and the suspension was quickly transferred to cylinders for settling tests with the rest of the procedures being the same.

After recording of settling heights, we waited for another hour prior to recording the turbidity of upper supernatant in the cylinder using turbiditimeter (HF Scientific, Inc. Water Analysis Instruments) and the height of final sediments. From the height and volume of the sediments and the weight of total solids settled, the solid content of the sediments can be calculated, which is another measure of settling performance. Different trends of ISR, turbidity and solid content determined are discussed below.

### 4.1.2 Relationship between ISR and Lime Concentrations for Anionic Flocculants

The settling results were divided into a number of graphs and each of the graph has the same concentration of MF336 as flocculants. Settling results of using lime supernatant and lime suspension are discussed separately (Figure 4.2 a-d).

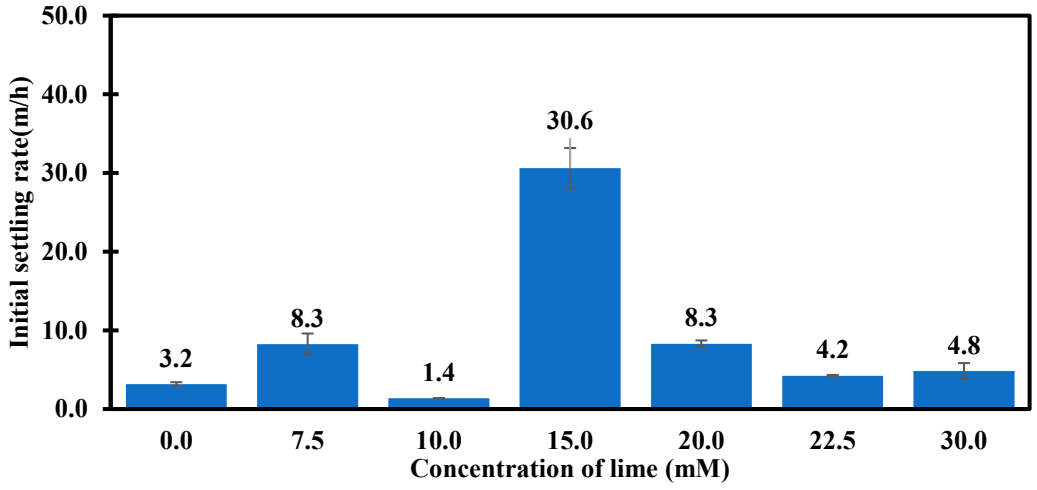


**Figure 4.2a Results of settling tests in lime supernatant with 2 ppm MF336**

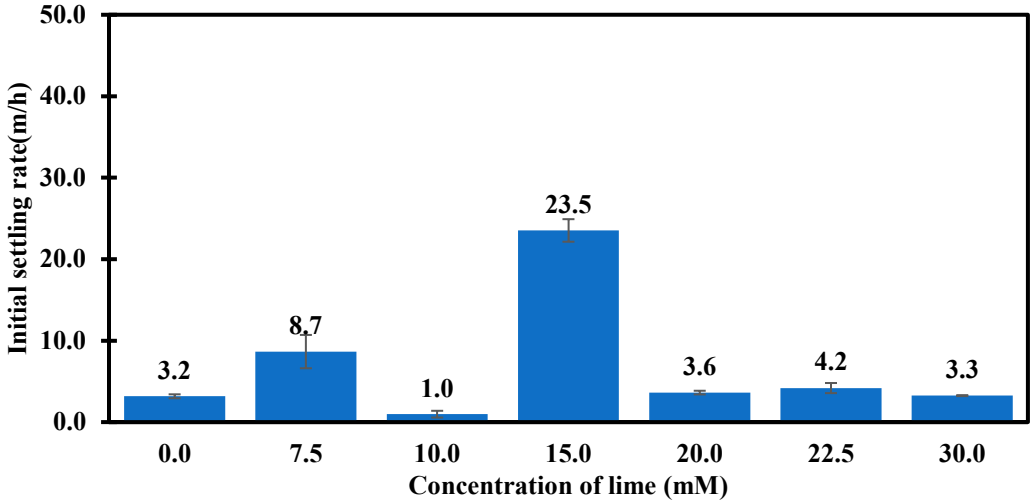


**Figure 4.2b Results of settling tests using lime suspension with 2 ppm MF336**

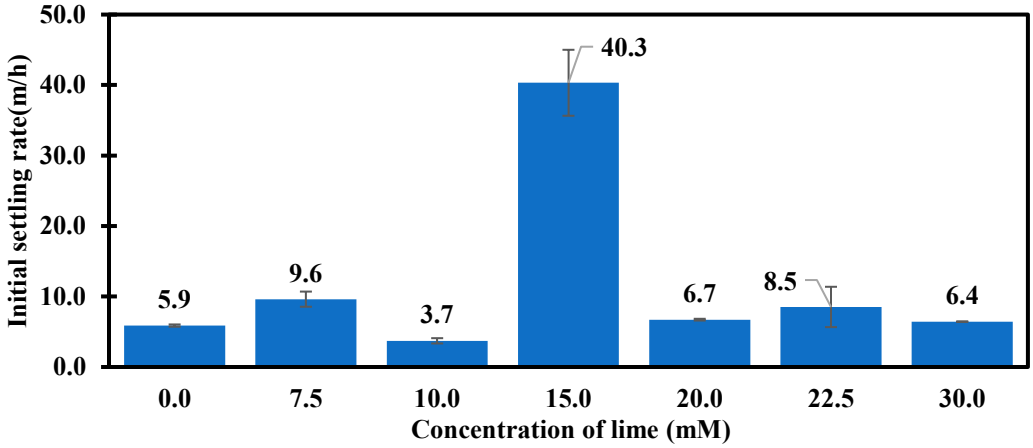


**Figure 4.2c Results of settling tests using lime supernatant with 3 ppm MF336**

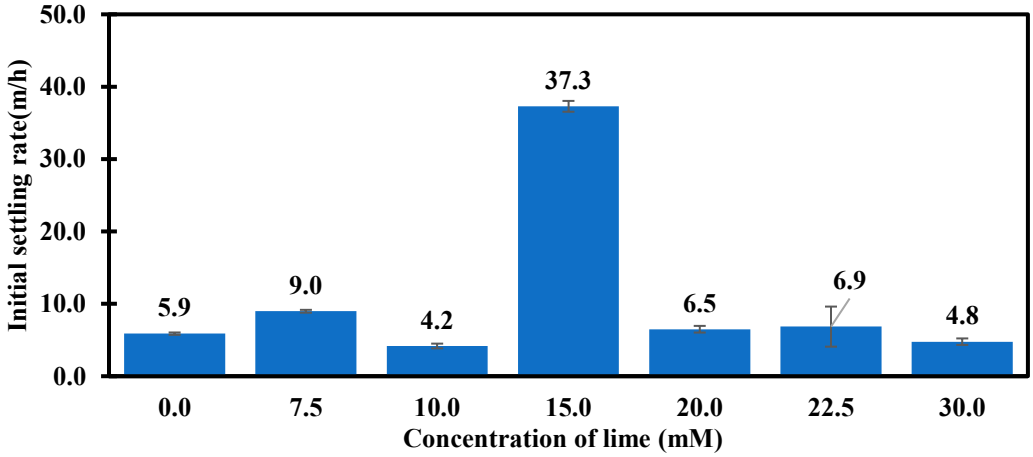


**Figure 4.2d Results of settling tests using lime suspension with 3 ppm MF336**

It can be seen from the results in Figures 4.2 a-d that the lime addition improves the initial settling rate significantly when its dosage is 15 mM . However, the ISR reduces with further increasing the lime dosage beyond 15 mM , indicating an overdose effect of lime addition. Clearly the optimal dosage of lime addition is 15 mM regardless the concentration of the polymer studied for both lime suspension and lime supernatant. Also an ISR reducing effect was found at the concentration of 10 mM, a possible explanation is that at the dosage where pH of the system is around 10.5 ~ 11, magnesium monohydroxide ions can precipitate out from the maximum concentration, according to the calculation in Chapter 5. Thus the adsorption of anionic polymers on the mineral surface is influenced, although further experiments in such concentration are needed to clarify the phenomena. Due to the lack of time and complexity of process water system, in this thesis there was no more experiments conducted regarding such concentration of lime and pH.

It is interesting to note that without or at low dosage (7.5 mM and 10 mM) of lime, a second mudline settling is observed, which is much slower than the first mudline descending. This is caused by insufficient amounts of polymer adsorption on the tailings particles, part of which form smaller flocs that settled at much slow rate to form the second mud layer on the top of the first layer in the cylinder. This second layer contains much less than 10% of the original MFT solids in the system. Only the first mudline ISRs are reported since the trends will not be changed and the mass of fine solids within the second mud layer is negligible.

Also the aqueous pH with each concentration of lime was recorded. As shown in Figure 4.3, the pH increased from the original pH of Aurora process water (8.3) to 11.89 with increasing lime addition up to 30 mM. The polymer dosage did not influence the pH. The existence of lime particles in the settling system did not influence the pH either.

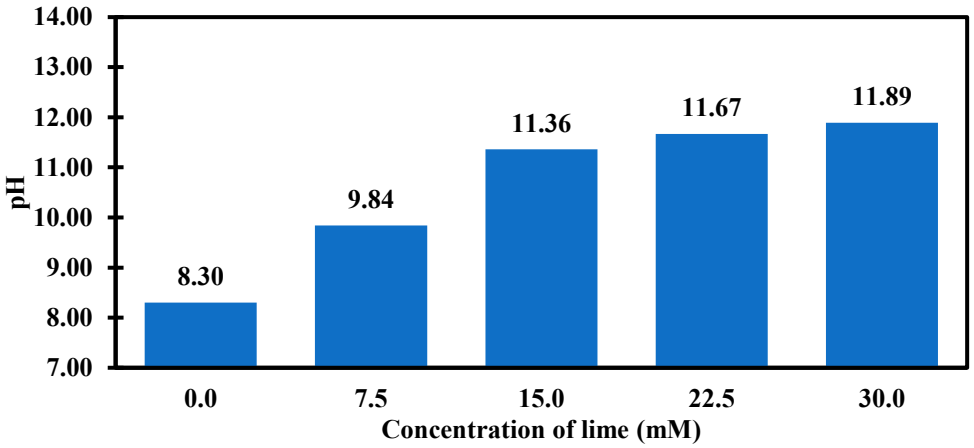


**Figure 4.3 pH at various concentration of lime**

4.1.3 Relationship between ISR and Polymer Concentrations for Anionic Polymers

Without lime addition, the settling performance is improved by polymer addition, reaching the optimal dosage of 0.7 g/ton on solids basis as shown in Figure 4.1. The addition of lime does not change this trends as shown in Figures 4.4 to 4.5. The ISRs with the intermediate concentration (15 mM) and high concentration (30 mM) of lime added as supernatant are shown in Figure 4.4 and 4.5 with increments of polymer concentrations. The ISRs with other dosages of lime added in lime supernatant and lime suspension follow the same trend.

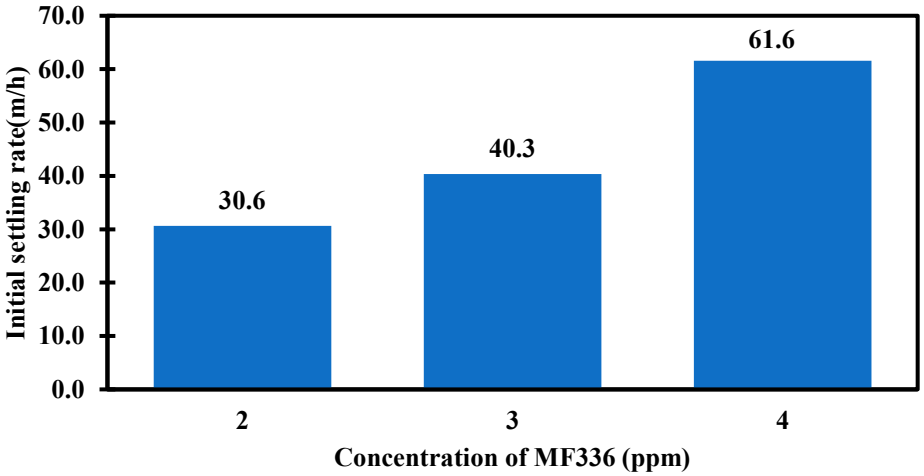


**Figure 4.4 Results of settling tests in 15 mM lime supernatant**

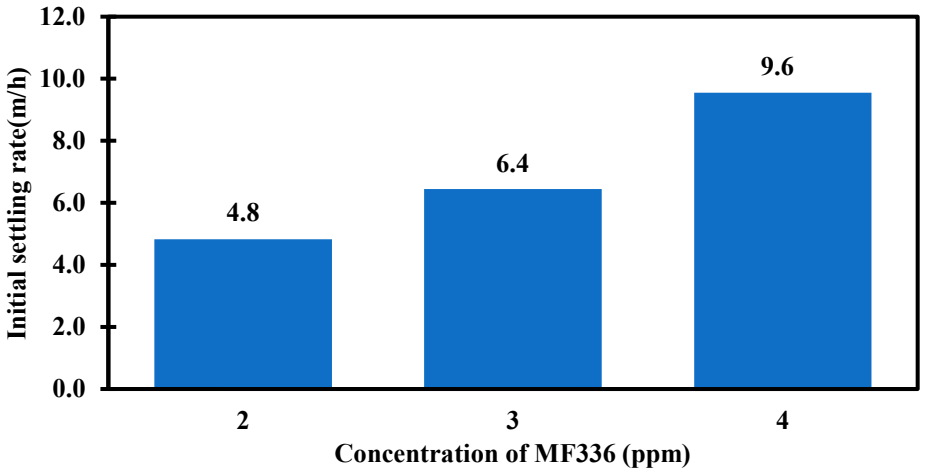


**Figure 4.5 Results of settling tests in 30 mM lime supernatant**

At optimal and excessive dosage of lime, increasing polymer concentration improved the ISR to different extends, which is possibly because the excessive amount of lime changes the conformations of the polymers and hinders the bridging effect with even higher concentrations of polymers. The details will be discussed in the next chapter.

4.1.4 Comparison of Results for Lime Supernatant and Lime Suspension with Anionic Polymers

As shown in Figure 4.11, the ISR using lime supernatant is higher than using lime suspension with visible lime particles at the same concentration of lime and the same concentration of MF336.

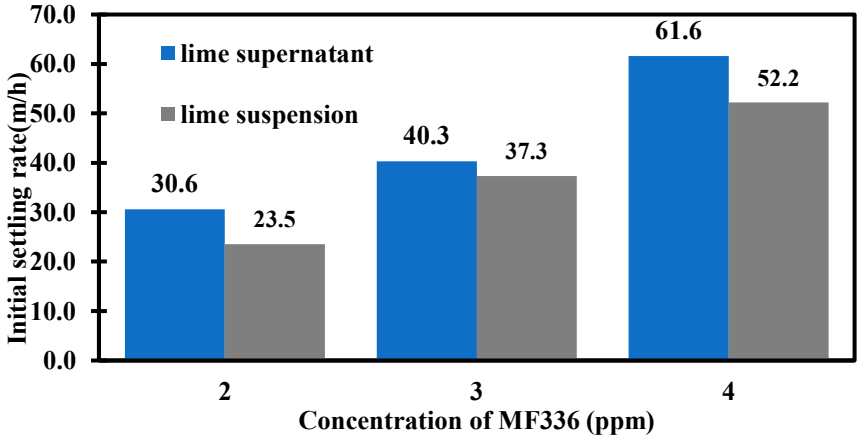


**Figure 4.6 Results of settling tests in 15 mM lime supernatant or suspension**

The intent of the experiments is to test the performance with unsolvable lime particles in the system, which does not require extra procedures and time for the premixed system to settle down and get the upper layer supernatant. Although it was observed that those particles reduced the settling performance.

The possible explanation is that the lime particles are also flocculated by polymers together with tailings particles. Those particles are later proven to be mainly $CaCO_3$, which will be discussed in the next chapter. The inert particles would probably not affect the interaction between tailings particles and polymers, although they could compete with tailings particles for flocculation. The particles have a higher PZC than tailings particles and tend to adsorb more anionic polymers. The polymers may collapse on the lime particles due to strong electrostatic attractions, decreasing the bridging effect. Thus the settling rate of solids in the suspension case is lower than in the supernatant case.

It is interesting to note that for most of the experiments, the final turbidity after 1 h settling is slightly lower when using lime suspension than using lime supernatant. It appears that the lime particles tend to attract more fine tailings particles by helping to form the sweep coagulation and hence to enmesh the settling tailings particles.

### 4.1.5 Influence of Lime Addition on Turbidity of Supernatant and Solid Content of Sediments

The turbidity of upper liquid in the cylinders and solid content percentage of sediments 1 h after initial settling were measured. Figures below show the results with varying concentrations of lime in supernatant at 0.2 kg/t MF336 dosage.

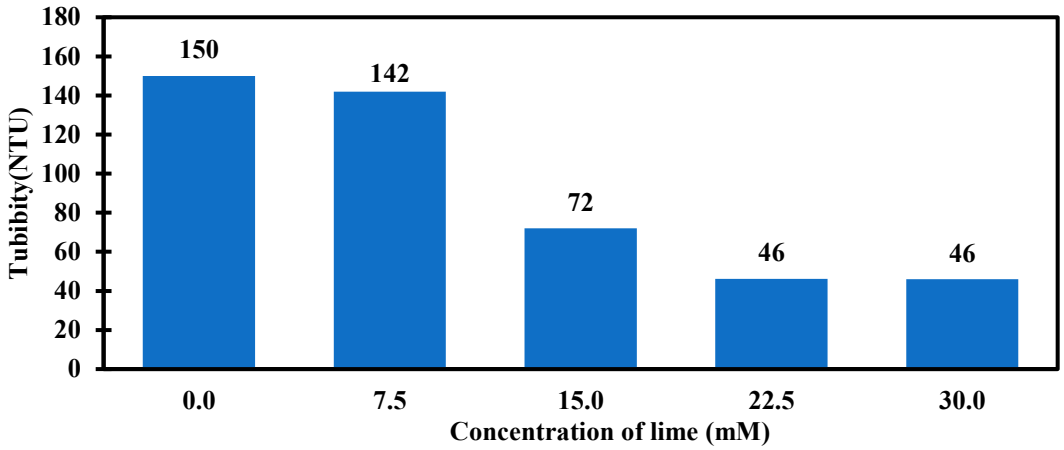


**Figure 4.7 Turbidity of supernatant of MFT with 2 ppm MF336 in lime supernatant**

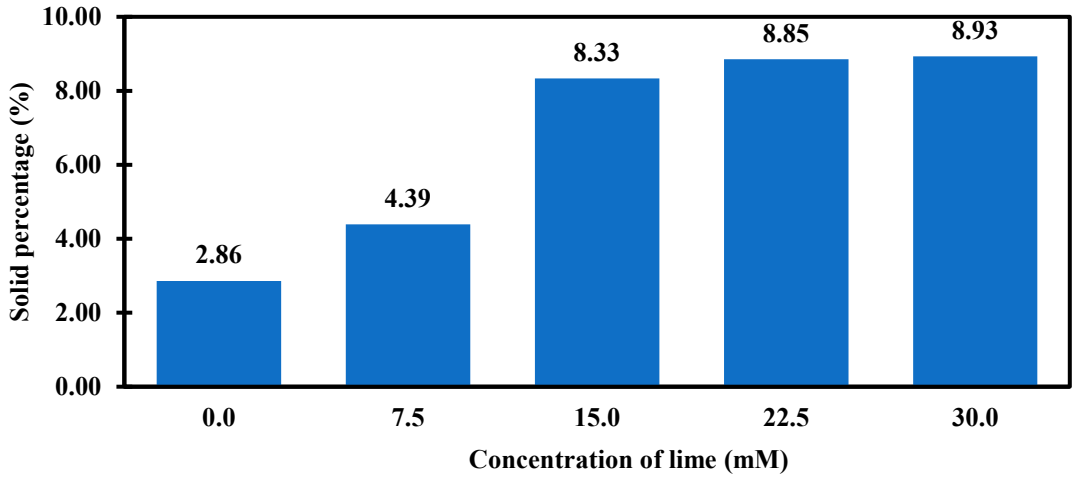


**Figure 4.8 Solid content in sediment of MFT with 2 ppm MF336 in lime supernatant**

The testing results with 3 and 4 ppm MF336 addition show the same trends. The turbidity decreased while the solid content in sediments increased with increasing the dosage of lime. Higher dosages of lime clearly help settle down fine particle through sweep coagulation thus reducing turbidity of the supernatant and increasing the solid content of sediments.

### 4.1.6 Settling Tests with Lime Supernatant and Cationic Flocculants

As in the settling tests using anionic flocculants, we hypothesize that the lime dosage could reverse the zeta potential of tailings particles from negative to positive. Because of the anionic polymers

used, the max adsorption would occur with the highest dosage of lime. But the max coagulation would occur at the intermediate dosage of lime where the zeta potential is the closest to zero. If this hypothesis is correct, the adsorption of cationic polymers is probably not going to be enhanced by the lime addition. We conducted settling tests with cationic polymers Zetag8110 over the same concentration range of lime.

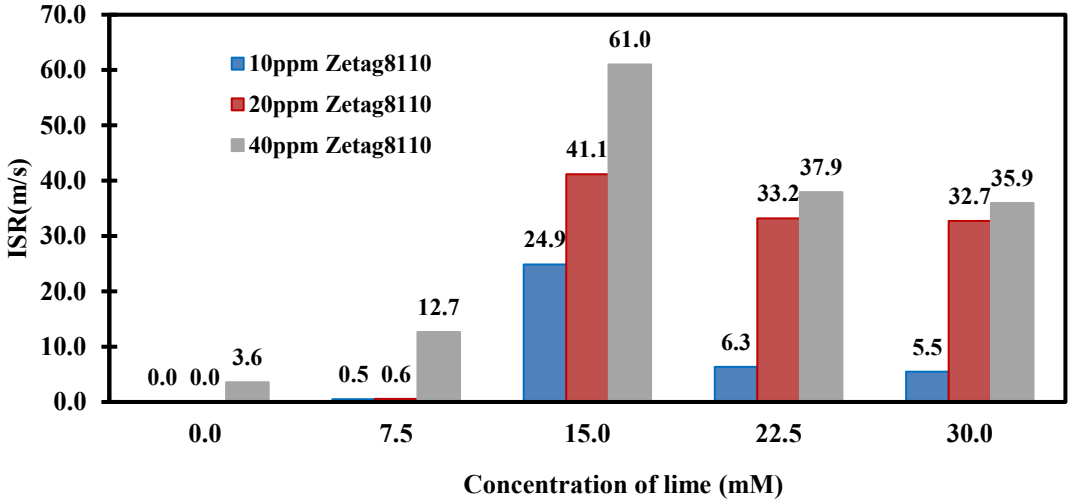


**Figure 4.9 Results of settling tests with Zetag8110 and lime supernatant**

Surprisingly, lime usage also enhanced the flocculation by cationic polymers significantly as shown in Figure 4.9. The ISR also experienced a decay at high dosages of lime. In order to find the proper explanation of how lime influences the adsorption of anionic/cationic polymers on originally negatively charged surfaces, it is needed to detect the surface potentials of the particles and the adsorption of polymers. To have a better understanding on the role of lime in flocculation of MFT particles, more settling tests were conducted with calcium from different sources under controlled pH by hydroxide additions.

### 4.1.7 Settling Tests with $CaCl_2$ and Anionic Flocculants

$CaCl_2$ is a type of water soluble calcium salts. $CaCl_2$ was added to process water before diluting MFT and flocculation. Since the chloride ions do not react with other species or participate in any adsorption process on the tailings particles while the screening effect of $Cl^-$ is not as significant as other divalent ions such as $Ca^{2+}$ or $SO_4^{2-}$ in PW, the results obtained could be considered to be influenced only by the addition of calcium ions. In Figure 4.10 the ISRs resulted from $CaCl_2$ and lime addition are compared at the same concentration of dissolved calcium in the system.

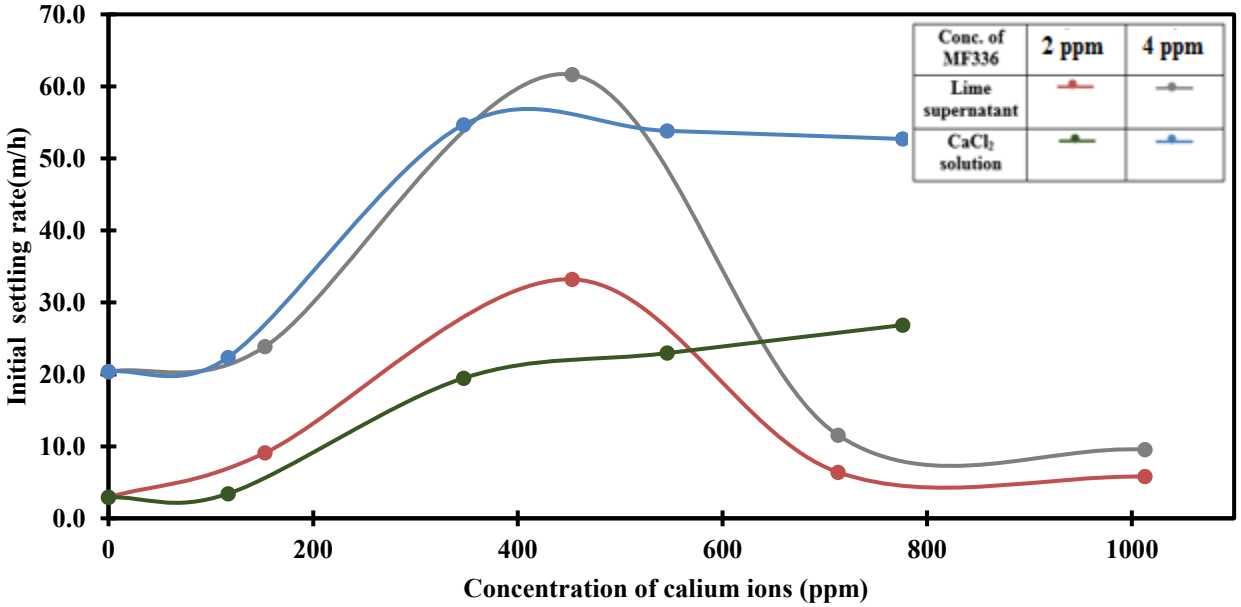


**Figure 4.10 Results of settling tests with calcium chloride or lime addition with MF336**

To obtain the dissolved calcium concentration in lime suspensions, we used ion chromatography to measure the upper layer of the supernatant, which will be discussed in the next chapter. As the results show, instead of having a best flocculation performance and a decay afterwards, the performances with pure calcium additions become a plateau beyond the intermediate dosage of calcium. The best performance is close to what we obtained using lime supernatant.

4.1.8 Settling Tests with NaOH and Anionic Flocculants

ISRs obtained using NaOH and lime before MF336 flocculation were compared. In this case, the system pH was used to represent the parallel axis.

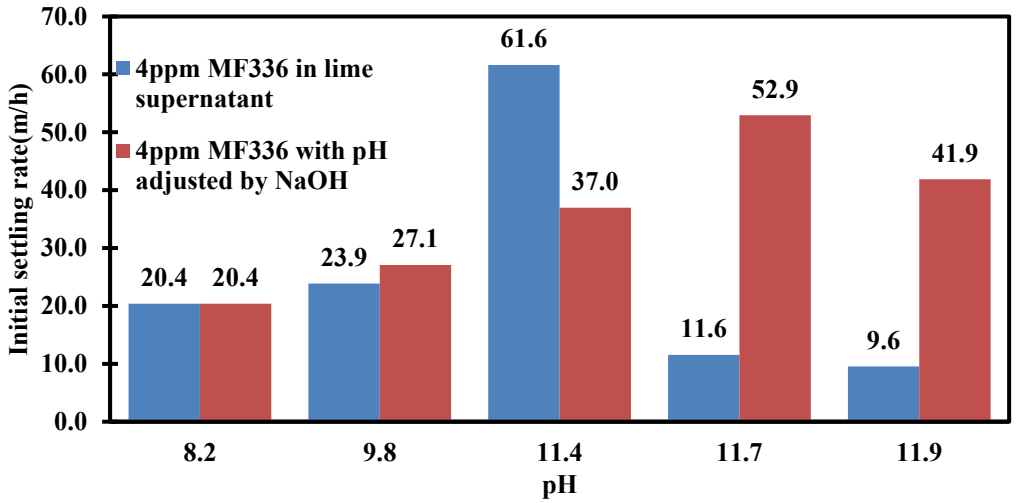


**Figure 4.11 Results of settling tests using 4 ppm MF336 with lime or NaOH addition to reach the same pH**

The addition of NaOH also enhanced the flocculation of MFT by 4 ppm MF336 with the best performance in pH of 11.7 . It is critical to mention that such improvement was achieved due to the presence of a significant amount of calcium ions in Aurora PW. Thus adding NaOH can trigger a similar mechanism to influence the adsorption of MF336 and hence its flocculation.

4.2 Focused Beam Reflectance Measurement

In order to acquire further information on how the tailings particles change in the flocculation process in a micro scale, focused beam reflectance measurement was used to monitor the size changes of particles in the system as lime was added and then the addition of polymers to the diluted MFT. Instead of mixing lime in process water before diluting MFT as in the previous

settling tests, the lime powder was added after diluting MFT because the size change of particle aggregates caused by coagulation can thus be detected.

A stirring rate of 200 rpm was used for the initial coagulation and flocculation process. Under the slow stirring rate the differences of size change can be clearly observed at different dosages of lime. Then the stirring rate was turned up to 400 rpm to study the breakage (strength) of flocs.

4.2.1 FBRM Tests with Lime and Anionic Flocculants

In testing the particle size changes at five lime concentrations, 2 ppm MF336 was used as flocculants.

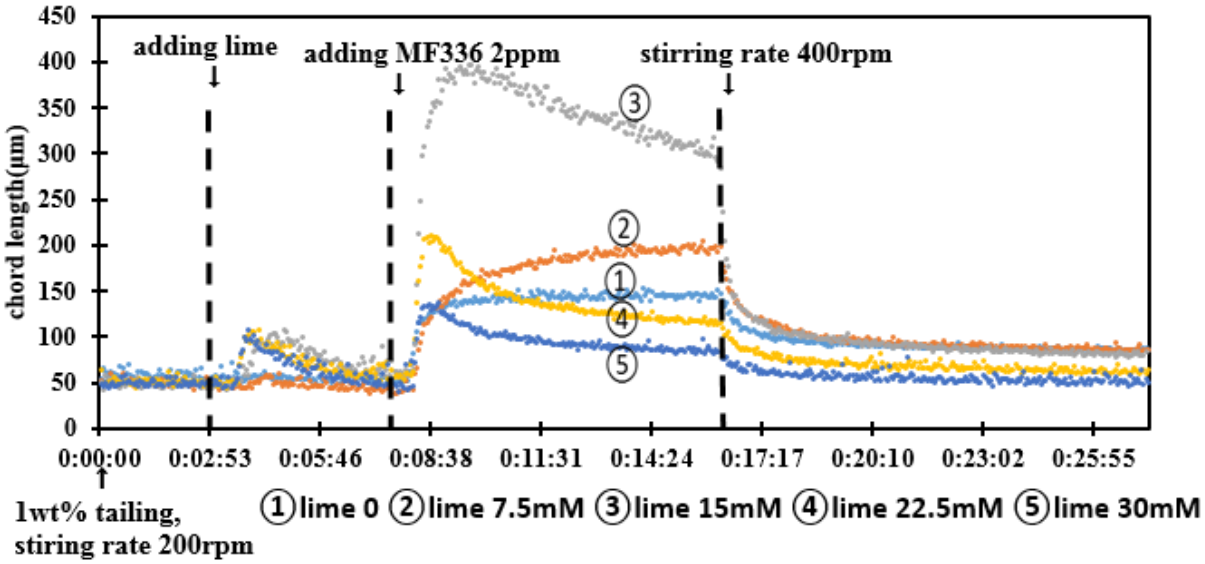


**Figure 4.12 Results of FBRM measurement for flocculation of 1% MFT using MF336 (2 ppm) and lime**

In the beginning of the measurements as shown in Figure 4.17, there was little change in particle size when 1wt% of MFT was stirred in a slow rate without any chemical addition. An obvious size shift was observed, corresponding to the coagulation caused by $Ca^{2+}$ from the lime with

concentrations from 15 mM to 30 mM. The rapidest and largest aggregation was observed with the highest dosage of lime tested. This was caused by the change in particle charges measured by zeta potential after adsorption of cationic calcium and calcium hydrolyzed ions on the tailings particles. The zeta potential increased probably to around 0 mV with 30 mM lime addition to achieve the largest coagulation. However, even in the slow stirring rate, the aggregation formed broke apart rapidly, which proves that aggregates formed by coagulation are much weaker than that formed by flocculation because of the weaker electrostatic forces in shorter ranges as compared with bridging effect.

After the tailings particles size stopped decreasing, 2 ppm of MF336 was added in a constant speed in 1 minute. The largest floc size was achieved in the lime concentration of 15 mM, corresponding to the highest ISR got in the settling tests. Thus the best flocculation performance enhanced by lime treatment was confirmed to be achieved at an intermediate dosage of lime and a decay of performance occurred at higher dosages of lime. This phenomenon is not caused by the coagulation mechanism because of the breakage of aggregates before the addition of flocculants.

It can be seen that breakage still occurred after adding flocculants in high lime concentration systems. After turning up the stirring rate, particles in all of the systems started to break apart to a similar size. The result indicates that adding pure inorganic salts such as lime to assist flocculation may not enhance the strength in a high shearing environment.

### 4.2.2 FBRM Tests with Lime and Cationic Flocculants

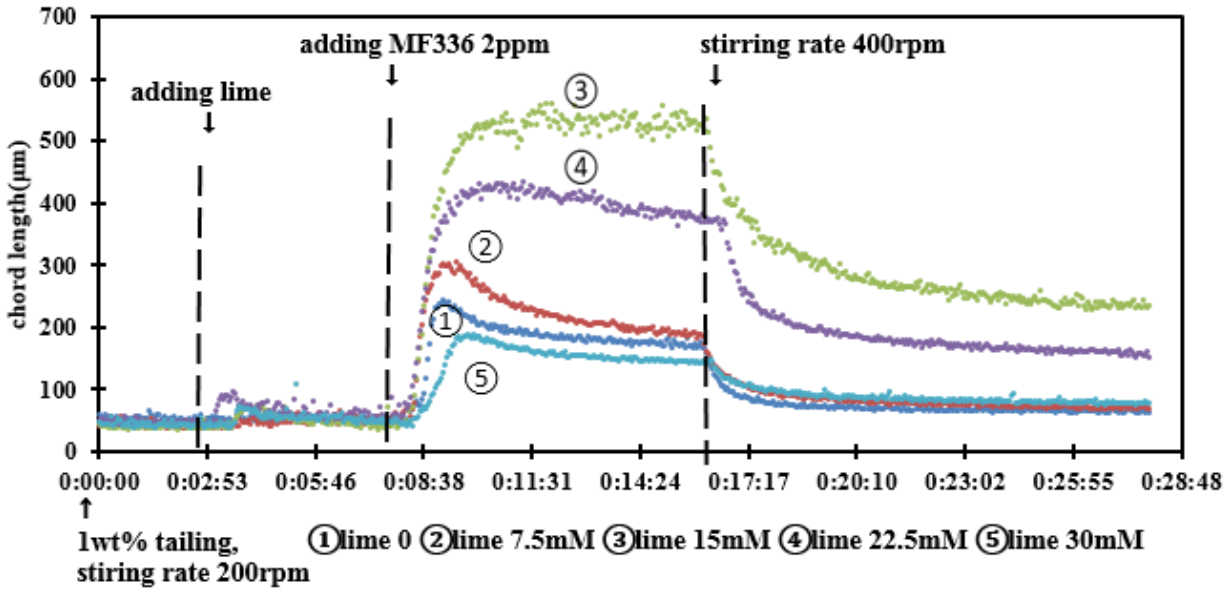


**Figure 4.13 Results of FBRM measurement for flocculation of 1% MFT using Zetag8110 (20 ppm) and lime**

Similarly small aggregates were formed after lime addition and then broke down almost immediately because of shearing. The largest floc size was observed at the intermediate dosage (15 mM) of lime, resulting in the highest ISR at the same concentration. The flocs slowly broke down after we turned up the stirring rate.

Similar to anionic polymer additions, cationic polymer flocculation is enhanced by lime mixed in the system. The floc size is drastically increased in intermediate dosage of lime addition. Under the strong mechanical shearing, the floc breaks down rapidly.

# Chapter 5 Mechanism Study

In order to explain the observations described in the previous chapter, several crucial characteristics of the materials used were studied. The mechanisms involved in the flocculation process were proposed. From the results of settling tests and floc size monitoring experiments obtained previously, the unique trend of performance influenced by lime addition indicates that the charge properties of mineral particles might be changed and even reversed by the changing water chemistry of the system. The zeta potentials which indicate the charge properties of the particle surfaces were first measured. The ion concentrations which are the main factors influencing the surface charges of particles in tailings were also measured. Next, a model system was established using Quartz Crystal Microbalance with Dissipation (QCMD) to estimate the adsorption of polymers on the tailings particles, which is influenced by the charge properties of particle surfaces. The configuration changes of the adsorbed polymers on the silica surfaces were recorded. By investigating the changes of both the amount of polymer adsorption and configurations, a clear point of view was established on how the flocculation performance is influenced by the lime addition with anionic/cationic flocculants.

## 5.1 Zeta Potentials of Tailings Particles

### 5.1.1 Changes of Zeta Potentials by Lime and NaOH Addition

Zeta potentials represent the surface charge properties of the tailings particles in our experiments. Zeta phoremeter (CAD) was used to measure zeta potential of MFT particles in Aurora Process Water at 0.1 wt% solid content. Before the measurement, PW was pre-mixed with lime for 2 h and settle down for 0.5 h. The upper layer supernatant with dissolved calcium ions and hydroxide ions

was used to dilute MFT. A portion of the resulting suspension was injected into the chamber of the zeta phoremeter for zeta potential measurement.

The measurements using the same procedures with only pH adjustment by NaOH addition in both Aurora PW and CNRL PW separately were also conducted for comparison. The results are shown in Figure 5.1. The lack of calcium in process water without lime addition leads to very different results. And by analyzing the results, we are able to explain the differences of the results in settling tests with lime and NaOH additions.

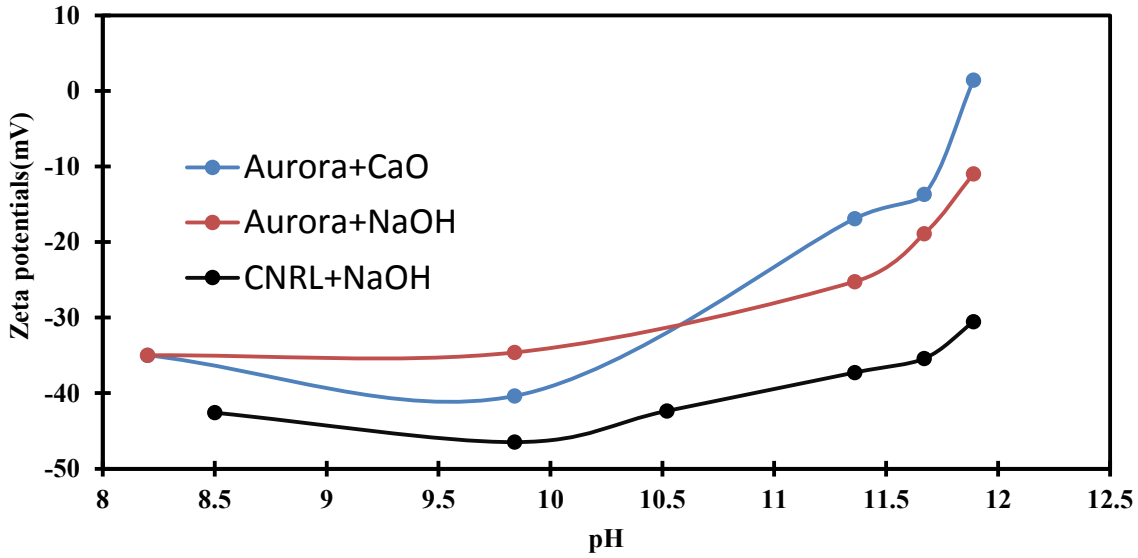


**Figure 5.1 Zeta potentials of MFT particles vs. pH of process water**

It should be noted that the pH of the measurements are approximately the same as the pH of the systems for settling tests and FBRM tests. As shown in Figure 5.1, the zeta potentials of particles in all three systems became less negative with increasing pH over the range studied by adding lime or NaOH. However, the zeta potential of the particles in Aurora PW system with lime addition increased more rapidly than that in Aurora water and CNRL PW with the pH adjusted by NaOH addition. The observed increment in zeta potential of fine particles with increasing pH contradicts

the general trend of decreasing zeta potential of fine particles with increasing pH. Such opposite trend is attributed to the presence of calcium ions in the system with stronger specific adsorption under increasing pH.

### 5.1.2 Effect of Lime Particles in Suspension on Zeta Potentials of Tailings Particles

From the results of settling tests reported in the last chapter, both calcium and hydroxide additions were shown to influence the flocculation process in PW. In the zeta potential measurement, we controlled the concentration of hydroxide ions by monitoring the pH. The only difference among the different systems is the concentration of calcium ions which determines the charge properties of the particles.

The concentration of ions in the original process water was measured by Ion Chromatography. The results for main ion concentrations are shown in Table 5.1 below:

**Table 5.1 Ion concentrations in Aurora and CNRL process water**

| conc.(ppm) | **$Na^+$** | **$K^+$** | **$Mg^{2+}$** | **$Ca^{2+}$** | **$Cl^-$** | **$SO_4^{2-}$** |
|---|---|---|---|---|---|---|
| Aurora | 876 | 15.75 | **12** | **27** | 432 | 333 |
| CNRL | 667 | 16 | **9** | **14** | 498 | 221 |

The main difference of the two process water is the concentrations of magnesium and calcium ions which are 33% and 50% higher in Aurora process water than in CNRL process water. The divalent ions can form hydrolyzed ions ($Mg(OH)^+$, $Ca(OH)^+$) which tend to attach to the mineral surfaces on metal oxide or metal hydroxide sites by hydrogen bond on basal siliceous surface and edge surface. Figure 5.2 shows possible types of specific adsorptions.

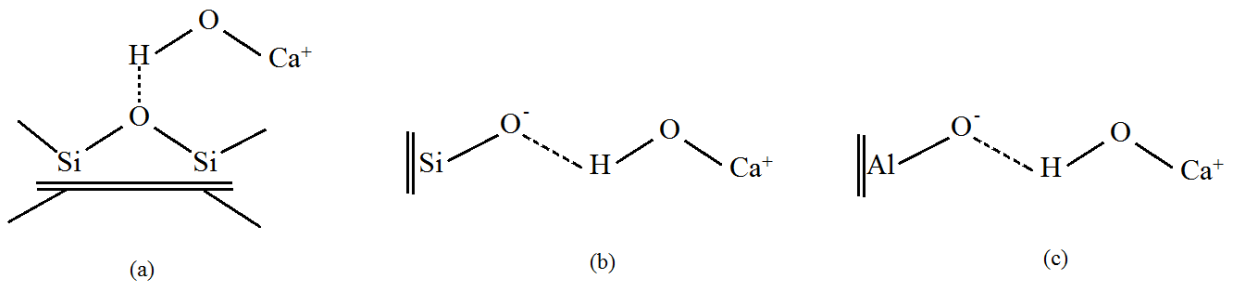


**Figure 5.2 Possible Types of Specific Adsorptions of Calcium Monohydroxide on Mineral Surfaces: (a) Basal siliceous surface and (b,c) Edge surfaces**

The data in Table 5.1 indicates that the higher zeta potentials of particles in Aurora PW is caused by the higher concentration of divalent cations. The concentration distribution of various calcium and magnesium species in the water are calculated from the hydrolysis reaction constant and solubility product of each ions given below.

$$Ca(OH)_2 \overset{Ksp}{\rightleftharpoons} Ca^{2+} + 2OH^- \qquad K_{sp} = 10^{-4.95}$$

$$CaOH^+ \overset{K}{\rightleftharpoons} Ca^{2+} + OH^- \qquad K = 10^{-1.28}$$

$$Mg(OH)_2 \overset{Ksp}{\rightleftharpoons} Mg^{2+} + 2OH^- \qquad K_{sp} = 10^{-10.61}$$

$$MgOH^+ \overset{K}{\rightleftharpoons} Mg^{2+} + 2OH^- \qquad K = 10^{-2.12}$$

All the constants are for room temperature (20 ºC) (Ekberg et al, 2016). MATLAB 2014a was used for calculating species concentrations as a function of pH from 7 to 14 with an interval of 0.01 and the results are shown in Figures 5.2 and 5.3.

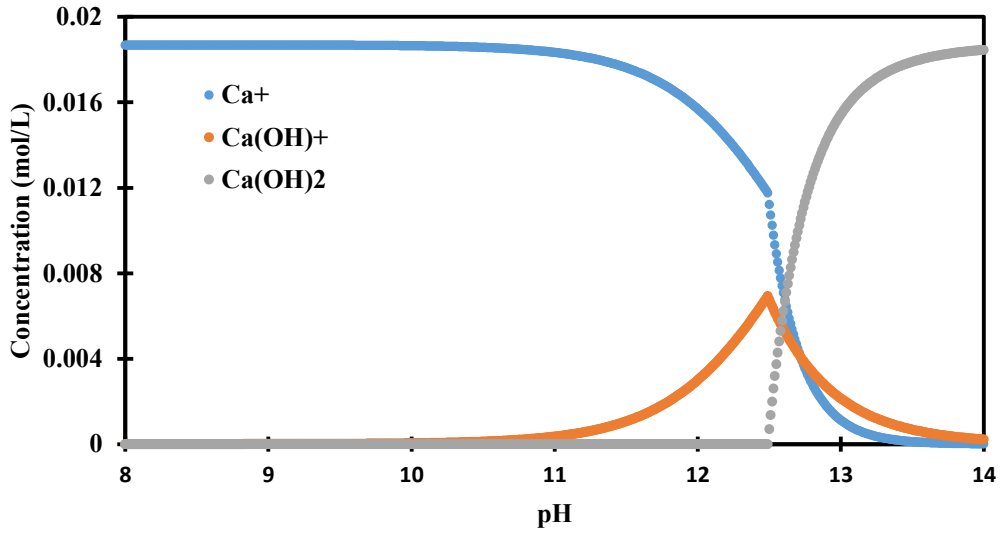


**Figure 5.3 Species Distribution of Calcium in Aurora Process Water**

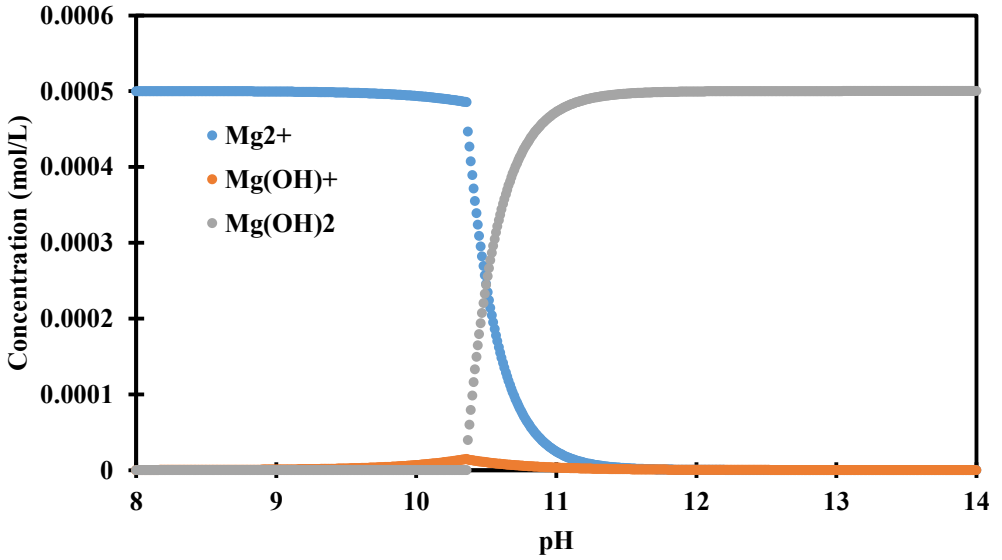


**Figure 5.4 Species Distribution of Magnesium in Aurora Process Water**

It can be seen from Figure 5.4 that most of the magnesium ions precipitate out before pH 11 and very few magnesium monohydroxyl ions are present as compared with calcium ions due to the

low solubility product of $Mg(OH)_2$. On the other hand, a substantial amount of calcium monohydroxyl ions are present between pH 11.5 and 13.5. The results of solution chemistry calculation suggest that calcium is the dominating species over magnesium in the experiments from pH 8 to pH 12. Increasing $Ca(OH)^+$ concentration with increasing pH by NaOH addition into the system led to increased adsorption of $Ca(OH)^+$ on the particle surfaces by specific adsorption mechanisms. For this reason, the zeta potential of the particles increased more rapidly in Aurora PW than in CNRL PW because of the larger amount of total calcium in the Aurora PW.

It is necessary to note that the reactions of calcium and $CO_2$ were not taken into consideration. In fact a significant amount of lime powder is converted into calcium carbonate after reacting with carbonate and bicarbonate ions in PW. TGA tests were conducted to analyze final components in the precipitates of lime suspensions later in this chapter. However the formation of $Ca(CO)_3$ does not influence the general conclusion on increasing $Ca(OH)^+$ with increasing pH, since $Ca(CO)_3$ is easier to form because it has a lower solubility product ($K_{sp} = 10^{-8.3}$) and the precipitates do not participate in any further reactions. A smaller amount of calcium will react with hydroxide ions and the actual critical pH where the concentration of $Ca(OH)^+$ reaches its maximum would be higher than the pH shown in Figure 5.3.

With the lime addition, the zeta potential increased most rapidly with increasing pH due to higher concentration of calcium added in the system to form more $Ca(OH)^+$. Ion chromatography was used to measure the soluble calcium species in the supernatant after mixing different amounts of lime in Aurora PW for 2 h and settling for 0.5 h.

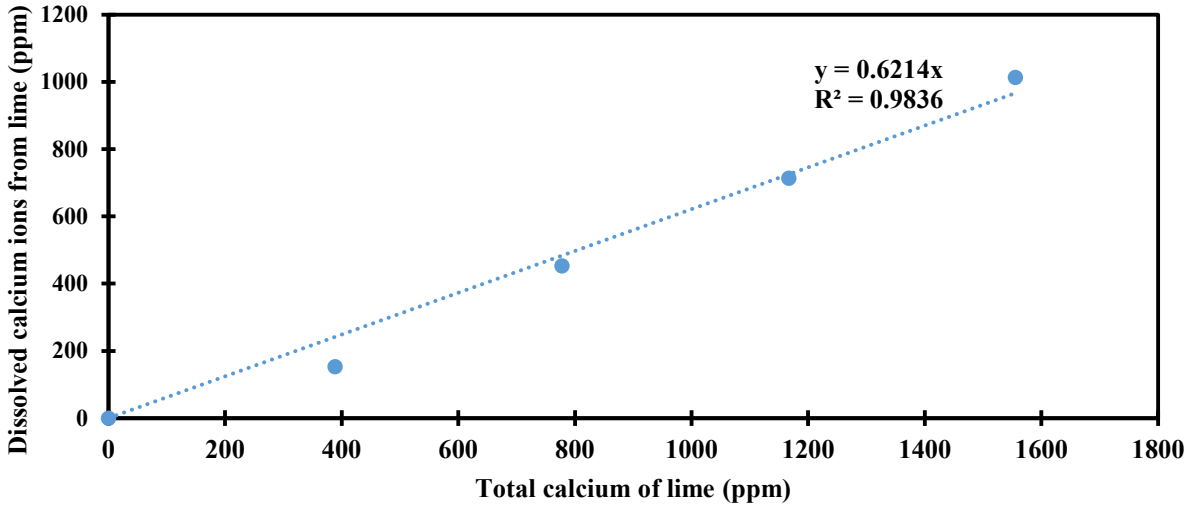


**Figure 5.5 Calcium ion concentration in lime supernatant measured by IC**

The results in Figure 5.5 show that around 62% of calcium from lime are in the soluble form and the rest forms the precipitates. For the highest dosage of lime used, 0.018 mmol/L of calcium can be dissolved in PW with a measured pH of 11.89, which should not generate $Ca(OH)_2$ precipitates according to the solubility product equilibrium.

To characterize the precipitates formed in the lime mixing procedure, TGA was used to measure the weight loss during the temperature rise in $N_2$ atmosphere from 20ºC to 800ºC. The weight loss changes of the samples are compared with those of the pure $Ca(OH)_2$ and $CaCO_3$ samples to determine the amount of $CaCO_3$(s) and $Ca(OH)_2$(s). The results are summarized in Table 5.2.

**Table 5.2 Components percentages of the precipitates after mixing lime in process water for 2 h**

| Lime addition (ppm) | $CaCO_3$ in precipitation | $Ca(OH)_2$ in precipitation |
|---|---|---|
| 544 | 80.75% | 2.80% |
| 1089 | 88.64% | 6.13% |

| | | |
|---|---|---|
| 1633 | 86.55% | 5.59% |
| 2178 | 83.77% | 4.56% |

Although there is no obvious trend for the $CaCO_3$ formation as the lime dosage increases, above 80 wt% of the precipitates formed is $CaCO_3$ and a very small part is $Ca(OH)_2$, which means that the precipitates of the system are mostly $CaCO_3$ formed by carbonate ions or $CO_2$ and $Ca^{2+}$ from lime. The unsolvable $CaCO_3$ is formed on the outer layer so that the small fraction of $Ca(OH)_2$ and the rest portion of the precipitates which is possibly CaO are surrounded inside and cannot further dissolve into the system. Because the main component of the precipitates is $CaCO_3$ rather than $Ca(OH)_2$, it further indicates that the system under pH of 12 is not saturated of $Ca(OH)_2$.

### 5.1.3 Changes of Zeta Potentials by $CaCl_2$ Addition

Various amounts of $CaCl_2$ were dissolved in Aurora PW containing around 0.1% MFT particles and the zeta potentials of tailings particles were measured using zeta phoremeter (Figure 5.6).

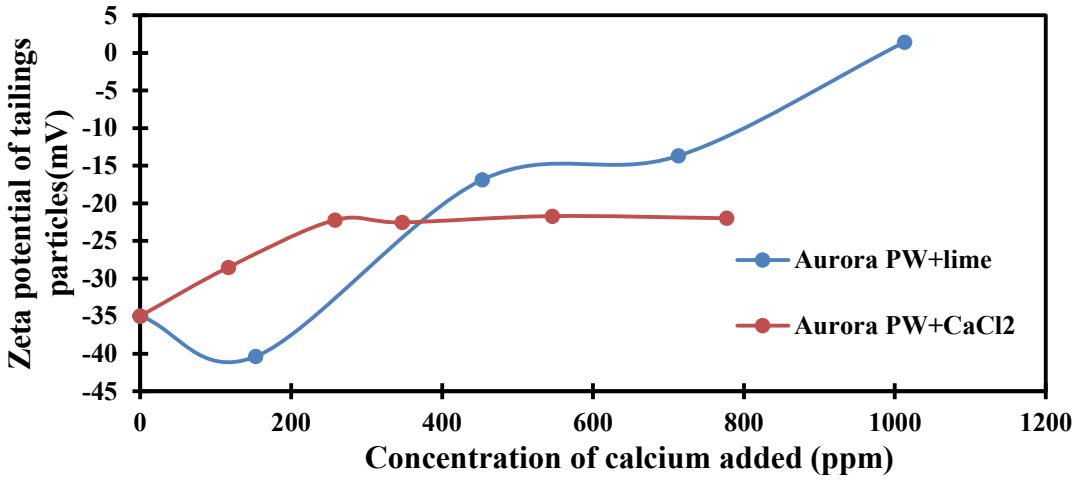


**Figure 5.6 Zeta Potentials of MFT particles as a function of $Ca^{2+}$ concentration from $CaCl_2$ addition and lime addition**

With the low dosage of $CaCl_2$ zeta potentials of the particles increased more rapidly than that with the lime additions for similar amounts of $Ca^{2+}$ addition. Beyond the intermediate dosage of $CaCl_2$ the zeta potentials do not further increase because without extra $OH^-$ added by lime, $OH^-$ in PW are mostly consumed by $Ca^{2+}$ to form limited amount of $Ca(OH)^+$, limiting the increase in zeta potentials caused by $Ca(OH)^+$ at around -20 mV. The pH of the system keeps around 7.3 ~ 7.5 after adding 300 ppm or more $CaCl_2$. The change of the zeta potential could explain the results in previous settling tests with $CaCl_2$ and MF336 where ISRs do not change significantly beyond the intermediate dosage of $CaCl_2$.

## 5.2 Measurement of Polymer Adsorptions and Analysis on Conformations of Adsorbed Polymers

Zeta potential changes have a great influence on adsorption of charged polymers on the particles. As discussed in the previous section, the zeta potentials of tailings particles increased from roughly -35 mV to 0 mV with calcium addition. As a result, the electrostatic repulsion between the tailings particles and the anionic polymer MF336 is reduced and the electrostatic attraction between the particles and the cationic polymer Zetag8110 is reduced. In another perspective, the higher ionic strength can screen the electrostatic interactions among the charged segments of the polymers. The conformations of polymer coils can be changed by changing the aqueous environment and charged state of the interfaces, both the factors influence the final bridging of particles by the adsorbed polymers and hence the flocculation performance.

In order to analyze the adsorption and the conformation changes of polymers on the interface, a quartz crystal microbalance with dissipation monitoring (QCMD) was used to detect the oscillation frequency and dissipation of quartz sensors coated with silica to adsorb polymeric flocculants in flowing liquid. The QCMD analysis is aimed to simulate the situation that flocculants are adsorbed

on the tailings particles surface with different concentrations of lime and surface potentials. $SiO_2$ was used as the coating materials to simulate the siliceous surface of tailings particles. Aurora PW with lime was mixed in the same ratios as used in the previous settling tests and zeta potential measurement. The supernatant without visible solid particles was mixed with polymer solutions at the ratio of 4:1 to obtain a designated concentration of polymers. The mixture is stirred by a magnetic mixer to ensure a uniform distribution. Then the solution of calcium and polymers in PW is directly pumped into the testing chamber of QCMD at a constant rate of 0.1mL/min and room temperature.

### 5.2.1 Results of QCMD Tests for Anionic Polymers

The concentration of MF336 is fixed at 60 ppm for each set of experiment in order to detect significant changes shown in Figures 5.6a, 5.6b, 5.6c and 5.6d.

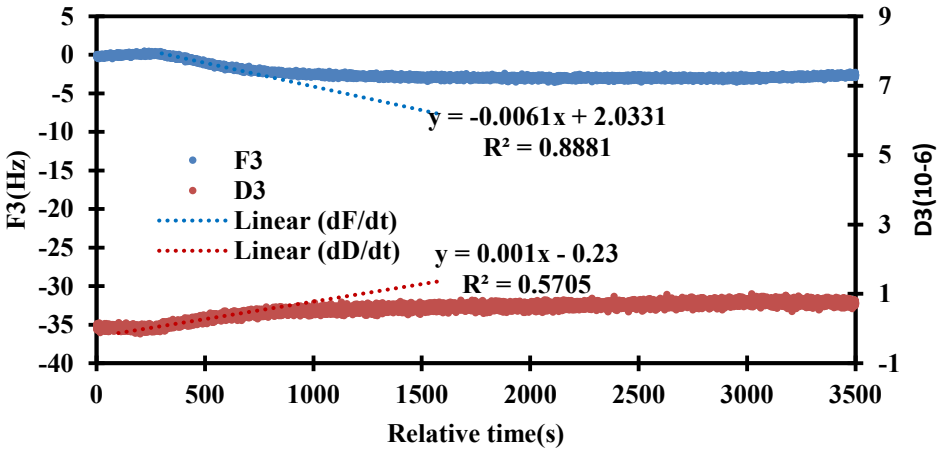


**Figure 5.7a MF336 adsorption on QCMD silica sensor in 7.5 mM lime supernatant**

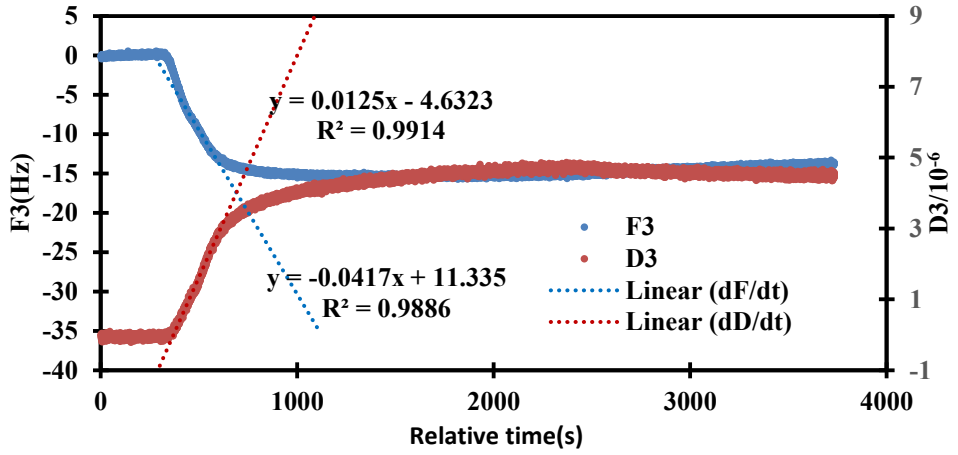


**Figure 5.7b MF336 adsorption on QCMD silica sensor in 15mM lime supernatant**

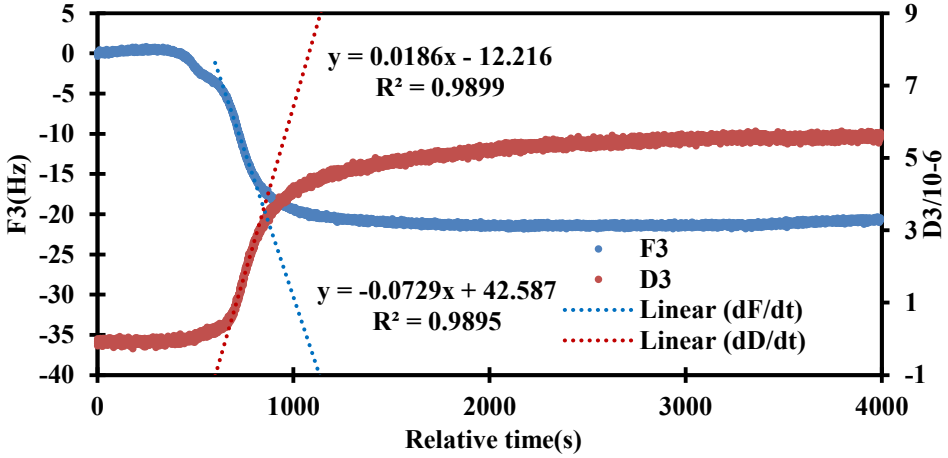


**Figure 5.7c MF336 adsorption on QCMD silica sensor in 22.5mM lime supernatant**

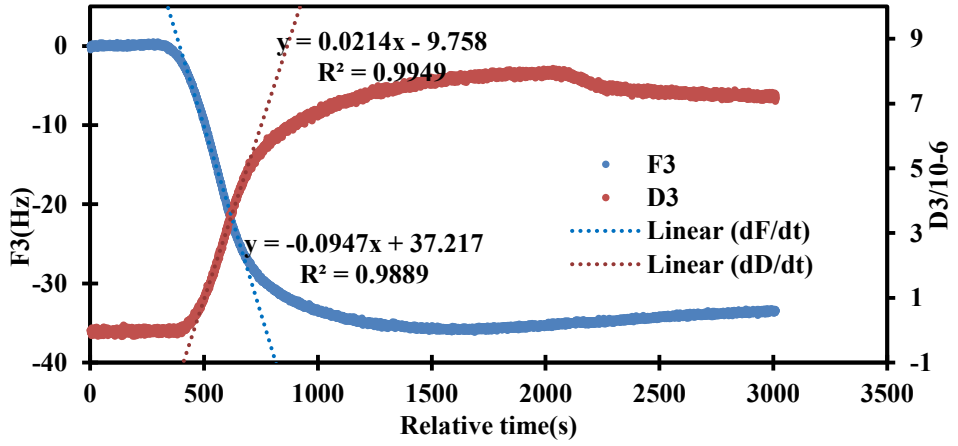


**Figure 5.7d MF336 adsorption on QCMD silica sensor in 30mM lime supernatant**

The frequencies and dissipations of QCMD silica sensors in polymer aqueous solutions of four different lime concentrations were recorded until the adsorption was nearly saturated. Only the frequency at the 3rd harmonic (F3) was recorded and analyzed. The frequency changes at other harmonics have the same trend.

As the results show, after around 500 s of the recording with the background solution, polymer solutions were allowed to flow through the tubes above the silica sensor surface. The adsorption caused the frequencies drop to different levels, depending on the lime concentrations used. The dissipations which represent viscous energy loss on the oscillating interfaces with polymers were increased accordingly. In order to understand the polymer conformational changes, initial slopes of the changes in the frequency and dissipation were calculated. The ratio of the dissipation change to the frequency change (dD/dF) shown in Figure 5.9 represents the viscous energy loss divided by mass of the first layer of adsorbed polymers on the interface, which provides a measure on the extension level the polymer chains.

The adsorption of polymers gradually reached the saturation state where the interface was fully covered. The final changes of frequencies and dissipations were recorded before the saturation. The ratios of the final changes of the frequency and dissipation ($\Delta D/\Delta F$) were calculated and the results are shown in Figure 5.9. Figure 5.8 shows the overall frequency shift in each set of the experiment in responding to polymer adsorption at different calcium dosages.

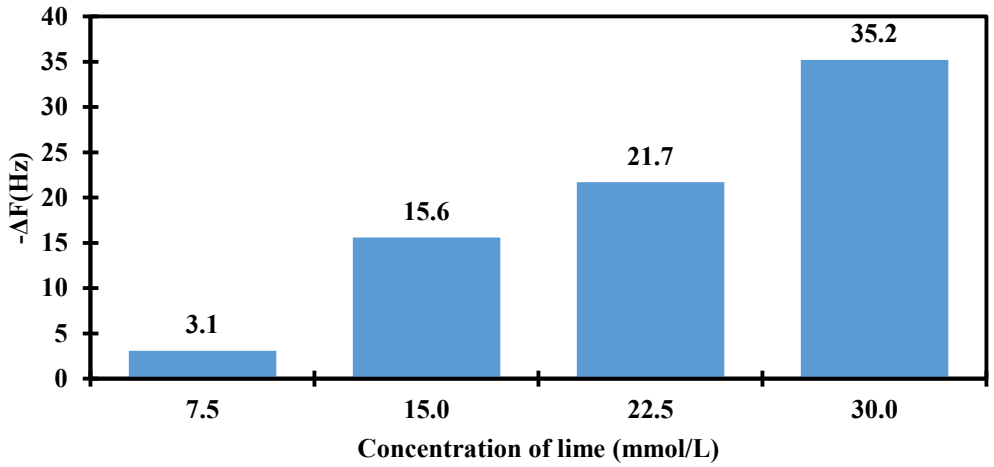


**Figure 5.8 Frequency shifts of 60 ppm MF336 adsorption on silica in lime supernatant**

There is no significant adsorption of MF336 on silica in QCMD tests of zero lime dosage. The final frequency change increases with increasing the lime addition, indicating an improved adsorption of the anionic polymer on the tailings particles because of the reduction in negative zeta potential of the particles by the lime addition. Another possible reason is the screening effect of electrostatic repulsion by high concentration divalent cations ($Ca^{2+}$) to allow more polymers to be attached on the interface by hydrogen bonding.

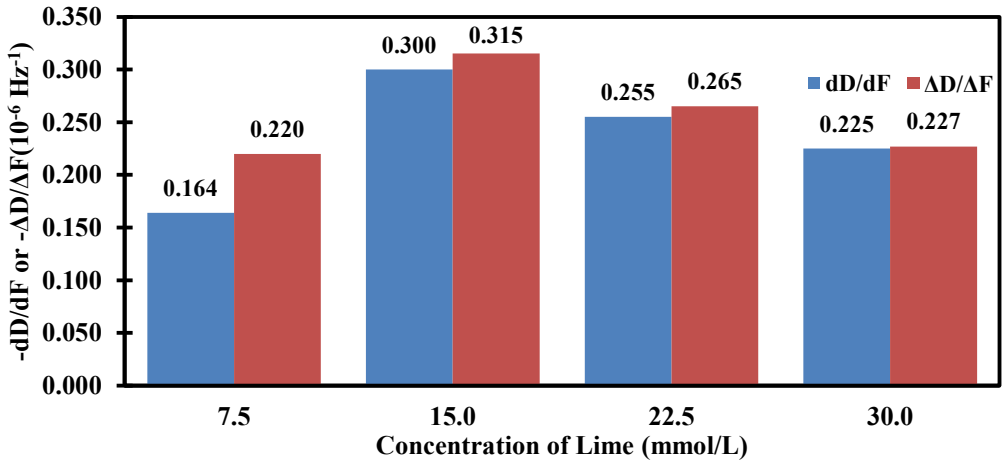


**Figure 5.9 Ratios of dissipation shifts to frequency shifts of MF336 adsorption on silica**

As shown in Figure 5.9, the maximum values for dD/dF and ΔD/ΔF are observed in the intermediate dosage of lime. This finding is consistent with the observed best flocculation performance with the same range of lime dosages.

Clearly there are complex conformational changes as the lime dosage are changed in PW. The viscous energy loss is low when high dosage of lime is used as a result of screening effect on the electrostatic repulsions between the segments of anionic polymers by higher concentration $Ca^{2+}$, leading to the more compact polymer coils. The adsorption of polymers on the interface is influenced by the zeta potential reduction and also the screening of electrostatic repulsion between polymers and solid particles. The polymers are adsorbed more easily on the interface to form a flatter layer which has less viscous interactions with liquid during the oscillation. Thus the bridging effect in the flocculation system can be largely eliminated by the conformation of adsorbed polymers, corresponding to the observed decrease of ISR and floc size at high lime dosage.

As shown in Figure 5.9, ΔD/ΔF and dD/dF follow the similar trends. However ΔD/ΔF is slightly higher than dD/dF in every set of experiments. The possible reason is that polymers adsorbed towards the equilibrium (ΔD/ΔF) are more extended away from the surface because of electrosteric interactions among the adsorbed polymers on the interface.

### 5.2.2 Results of QCMD Tests for Cationic Polymers

In the settling tests and FBRM measurement reported in previous chapter, lime addition was found to enhance the flocculation of MFT fine particles by cationic polymer. Here the adsorption of cationic polymer ZETAG8110 with increasing lime concentrations on the silica surface is determined qualitatively with the results shown in Figures 5.9a, 5.9b and 5.9c.

The QCMD measurement and analysis procedures are similar to that for anionic polymers except for dD/dF which is not recorded because of the non-linear initial change of dD and dF with adsorption time for the cationic polymers.

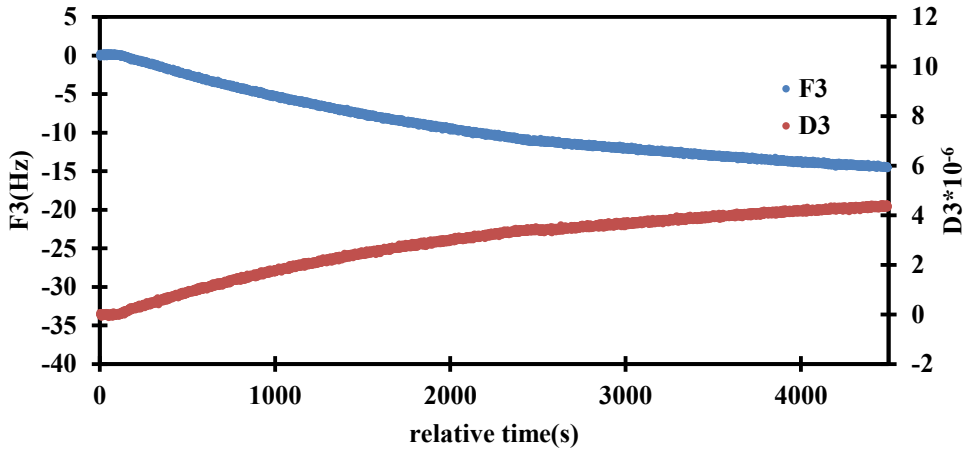


**Figure 5.10a Zetag8110 adsorption on QCMD silica sensor in 0 mM lime supernatant**

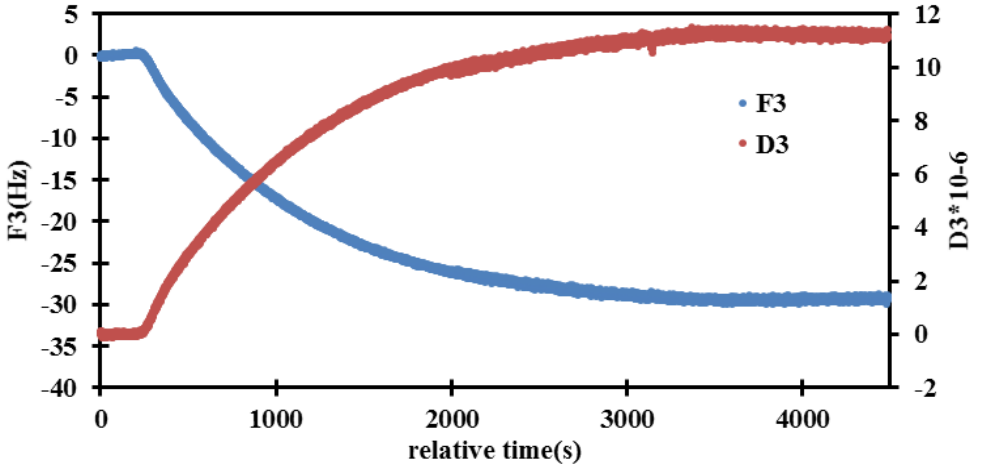


**Figure 5.10b Zetag8110 adsorption on QCMD silica sensor in 24 mM lime supernatant**

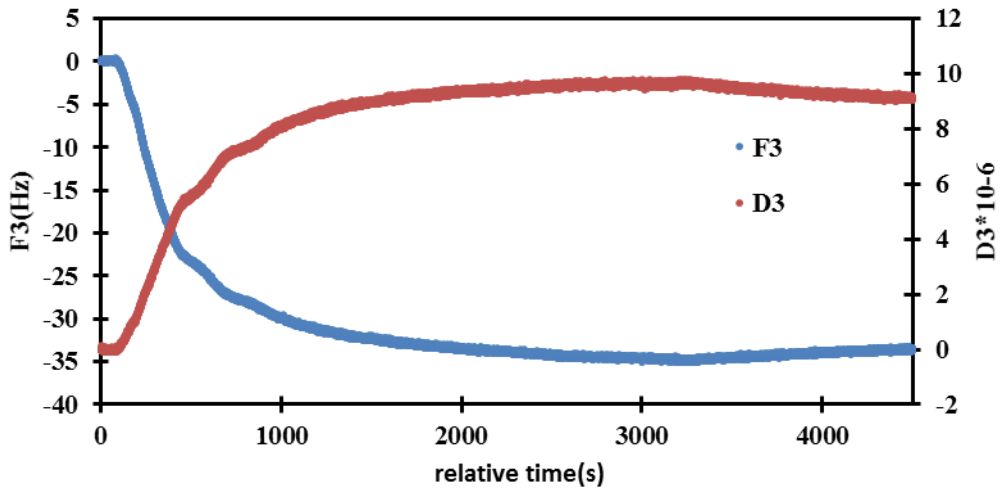


**Figure 5.10c Zetag8110 adsorption on QCMD silica sensor in 12mM lime supernatant**

Three concentrations of lime are tested with the fixed polymer concentration of 60 ppm. The frequency shifts and ΔD/ΔF are shown in Figures 5.10 and 5.11, respectively. As shown in Figure 5.11, a significant increase in adsorption amount of polymers with increasing lime addition was observed.

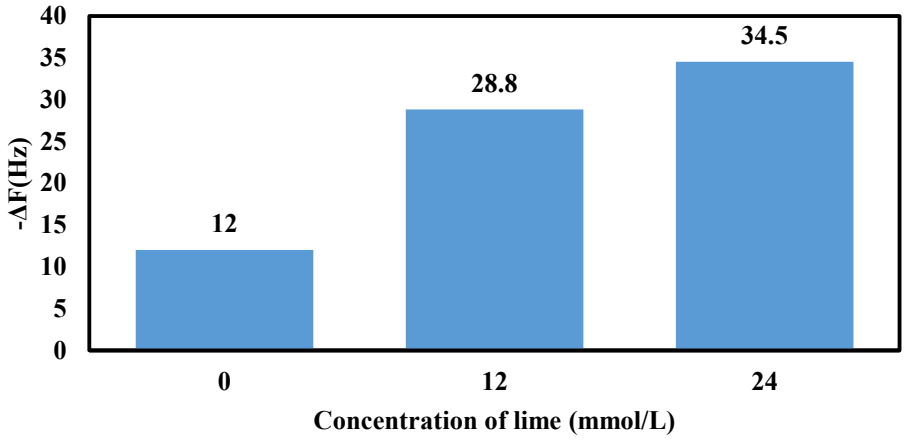


**Figure 5.11 Frequency shifts of 60 ppm ZETAG8110 adsorbed on silica (t = 3000s)**

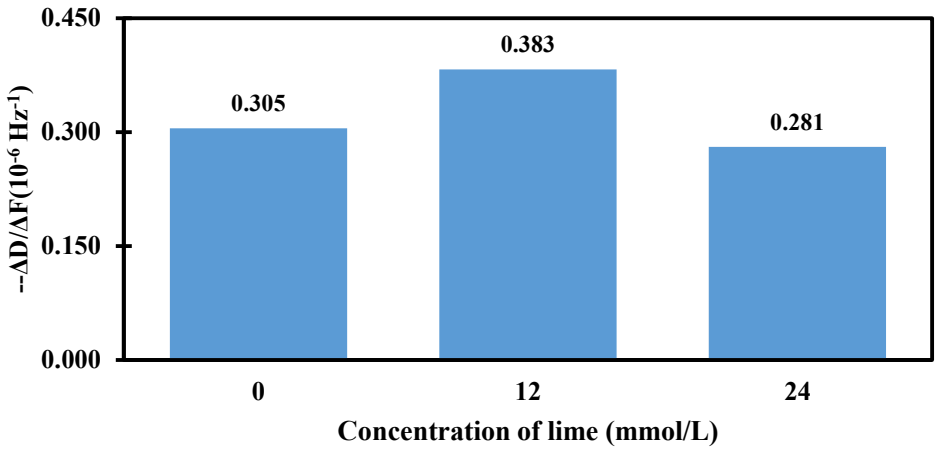


**Figure 5.12 Ratios of dissipations shifts to frequency shifts of ZETAG8110 adsorption on silica (t=3000s)**

The adsorption of polymers is enhanced as the concentration of lime is increased despite of the fact that the electrostatic attraction between silica surface and cationic polymers are reduced by the screening effect of calcium ions and the decreased zeta potential of the surface. As a moderately charged cationic polymer, ZETAG8110 can have extensive conformations in the aqueous environment, which hinders the adsorption process onto the silica surface because of the steric effect. The high calcium concentration may screen the repulsions between charged segments so that the surface will adsorb more compact polymer coils as illustrated by the screening enhanced regime introduced in chapter 2. However, at the high dosage of lime, the polymers become less extensive and form fewer loop and tail structures which reduce the bridging effect.

The dissipation factor of the adsorbed polymers shows a complex trend where the largest dissipation (most extensive conformations) was found at the intermediate dosage of lime. This observation indicates that the conformations of polymers close to the charged surface are also influenced by the electrostatic attraction between the polymers and the surface. With low concentrations of lime, the highly negatively charged silica surface may facilitate the formation of

a more compact adsorption layer with fewer loop and tail structures. The highest $\Delta D/\Delta F$ found in the intermediate dosage of lime indicates the high extensiveness of flocculation by the adsorption polymer. Such extended conformation of the adsorbed polymer results in a significant bridging effect of flocculation as shown by improved settling and increased size of flocs measured by FBRM for cationic flocculants at the intermediate dosage of lime addition.

# Chapter 6 Conclusions and Future Work

The settling tests and FBRM measurements showed that the flocculation by both anionic and cationic polymers is improved by premixing lime and process water before MFT dilution. The highest ISR and largest average floc size were found at the intermediate dosage (15 mmol) of lime for both types of charged polymers. A decay of the flocculation performance was observed at higher dosage of lime as shown by lower ISR and smaller floc sizes. An irregular trend of ISR was also found in the range from low dosage (5 mmol) to intermediate dosage (15 mmol) of lime, which is possibly a result of precipitated magnesium concentration in the range of pH changed by lime.

A further study on the surface charge property of the tailings particles and the water chemistry shows that increase in calcium ions and calcium monohydroxide ions with increasing lime dosage increases zeta potentials of the particles from negative to nearly 0mV by specific adsorption of calcium monohydroxide ions. Such reduction or neutralization of surface charges causes weak coagulation of tailings particles. The aggregates formed as such can be easily broken down. Magnesium existing in process water can also form monohydroxide ions with very low dosage of lime, however it can be totally precipitated out beyond pH of 11.

The increase in zeta potentials of tailings particles with lime addition enhances the adsorption of both anionic and cationic polymers but with different mechanisms. The high concentration of divalent cations in the system and the electrostatic interaction between the surface and polymer chains influence the conformations of adsorbed polymers. The adsorption process was analyzed qualitatively by QCMD measurements. At high dosage of lime, the adsorbed layer of polymer on the silica surface has the most compact conformation for both anionic and cationic polymers,

which leads to reduced bridging effect in the flocculation and explains the results of our cylinder settlings test and FBRM measurements. Overall a proper use of lime could reduce the dosage of polymers to achieve similar or better flocculation performance for both cationic and anionic polymers studied.

For recommended future work, an interesting phenomena was observed when a proper amount of lime was directly added into undiluted MFT: the resulted MFT formed a paste-like structure encapsulating water content, which has an extremely high shear strength and resistance to deformation by external forces (volute screw press). The resultant can dry out to a solid state by water evaporation in room temperature in several days based on the ratio of total surface area to total volume. The paste-like structure can be explained by geopolymerization mechanism in which aluminosilicate minerals in alkaline environment can be connected by hydrogen bonds on mineral surface. Previous researchers have studied such reactions on oilsands tailings (Rao et al, 2015; Nusri et al, 2016) although kaolinite and sodium hydroxide was used resulting in weak structure solidification with complicated preprocessing steps including flocculation. Further research is suggested here to study on the role of calcium from lime in geopolymerization reactions resulting in strong paste-like structures.

Also QCMD measurement with different types of sensor surfaces to simulate the structure of oil sands tailings surfaces should be conducted. The order of adding polymeric materials and inorganic salts into the fluid flow can be alternated to better simulate the procedures of the cylinder setting tests. Computational work should be conducted for the polymer adsorption on the minerals in different water chemistries in the research above.

# References


Alamgir, A.; Harbottle, D.; Masliyah, J.; Xu, Z.; Al-PAM assisted filtration system for abatement of mature fine tailings. *Chemical Engineering Science* 2012, 80 91-99

Atesok, G.; Somasundaran, P.; Morgan, L.J. Adsorption properties of $Ca^{2+}$ on Na-kaolinite and its effect on flocculation using polyacrylamides. *Colloids and Surfaces* 1988, 32 127-138

Basu, S.; Nandakumar, K.; Masliyah, J. On bitumen liberation from oil sands. *The Canadian Journal of Chemical Engineering* 1997, 75(2) 476-479

Berg, J.C. An Introduction to Interfaces and Colloids: The Bridge to Nanoscience. *World Scientific* 2010

Bockris, J.O'M.; Devanathan, K.; Müller, K. On the structure of charged interfaces. *Proceedings of the Royal Society A* 1963, 274(1356) 55-79

Boström, M.; Deniz, V.; Franks, G.V.; Ninham, B.W. Extended DLVO theory: Electrostatic and non-electrostatic forces in oxide suspensions. *Advances in Colloid and Interface Science* 2006, 123(1) 5-15

BP Statistical Review of World Energy. *BP Global* 2016 (url: www.bp.com/en/global/corporate/energy-economics/statistical-review-of-world-energy.html)

Chen, F.; Finch, J.A.; Xu, Z.; Czarnecki, J. Wettability of fine solids extracted from bitumen froth. *Journal of Adhesion Science and Technology* 1999, 13(10), 1209-1224

Cuddy, G. Oil sands geology. Guest lecture notes for Chemical Engineering 534, Fundamentals of Oil Sands Extraction, University of Alberta 2004

Derjaguin, B.; Landau, L. Theory of the stability of strongly charged lyophobic sols and of the adhesion of strongly charged particles in solutions of electrolytes. *Acta Physico Chemica URSS* 1941, 14 633-662

Derjaguin, B.V.; Churaev, N.V.; Muller, V.M. The Derjaguin—Landau—Verwey—Overbeek (DLVO) Theory of Stability of Lyophobic Colloids. Chapter 8 of Surface Forces. *Springer Science and Business Media New York* 1987

Directive 074 SUSPENDED - Tailings performance criteria and requirements for oil sands mining schemes. *Alberta Energy Regulator* 2009

Directive 085 Fluid tailings management for oil sands mining projects. *Alberta Energy Regulator* 2017

Dobias, B.; Stechemesser, H. Coagulation and Flocculation: Second Edition, 2nd ed., *CRC Press* 2005

Dukhin, A.S.; Goetz, P.J. Ultrasound for Characterizing Colloids. *Dispersion Technology, Inc.* 2002

Ekberg, C.; Brown, P.L. Hydrolysis of Metal Ions, *Wiley-VCH Verlag GmbH & Co. KGaA* 2016

Feng, X.; Mussone, P.; Gao, S.; Wang, S.; Wu, S.; Masliyah, J.; Xu, Z. Mechanistic study on demulsification of water-in-diluted bitumen emulsions by ethylcellulose. *Langmuir* 2010, 26(5) 3050-3057

Gardner, K.L.; Murphy, W.R.; Geehan, T.G. Polyacrylamide solution aging. *Journal of Applied Polymer Science* 1979 22(3) 881-882

Garrett, R.H.; Grisham, C.M. Biochemistry (4th Edition). *Brooks/Cole, Cengage Learning* (2010)

Grahame, D.C. The electrical double layer and the theory of electrocapillarity. *Chemical Reviews* 1947, 41(3) 441-501

Gregory, J. Polymer adsorption and flocculation in sheared suspensions. *Colloids and Surfaces* 1988, 31 231-253

Guo, C. Rapid Densification of the Oil Sands Mature Fine Tailings (MFT) by Microbial Activity. Ph.D. Thesis, University of Alberta 2009

Gurrmoorthy, A.V.P.; Khan, K.H. Polymers at interfaces: Biological and non-biological applications. *Recent Research in Science and Technology* 2011, 3(2) 80-86

Hamilton, J. A Glut of Oil? *Econbrowser* 2014 (url: http://econbrowser.com/archives/2014/11/a-glut-of-oil)

Harbottle, D.; Chen, Q.; Moorthy, K.; Wang, L.; Xu, S.; Liu, Q.; Sjoblom, J.; Xu, Z. Problematic stabilizing films in petroleum emulsions shear rheological response of viscoelastic asphaltene films and the effect on drop coalescence. *Langmuir* 2014, 30(23) 6730-6738

Hiemstra, T. Variable charge and electrical double layer of mineral–water interfaces: silver halides versus metal (hydr)oxides. *Langmuir* 2012, 28(44) 15614-15623

Hunter, R.J. Zeta Potential in Colloid Science: Principles and Applications. *Academic Press Inc.* 1981

James, R.O.; Healy, T.W. Adsorption of hydrolyzable metal ions at the oxide—water interface. I. Co(II) adsorption on $SiO_2$ and $TiO_2$ as model systems. *Journal of Colloid and Interface Science* 1972, 40(1) 42-52

Jiang, J. The role of coagulation in water treatment. *Current Opinion in Chemical Engineering* 2015, 8 36-44

Jiang, T.; Hirasaki, G.J.; Miller, C.A.; Ng, S. Effects of clay wettability and process variables on separation of diluted bitumen emulsion. *Energy and Fuels* 2011, 25(2), 545-554

Jiang, T.; Hirasaki, G.J.; Miller, C.A.; Ng, S. Wettability alteration of clay in solid-stabilized emulsions. *Energy and Fuels* 2011, 25(6), 2551-2558

Konan, K.L.; Peyratout, C.; Bonnet, J.-P.; Smith, A.; Jacquet, A.; Magnoux, P.; Ayrault, P. Surface properties of kaolin and illite suspensions in concentrated calcium hydroxide medium. *Journal of Colloid an Interface Science* 2007, 307(1) 101-108

Kumar, K.; Nikolov, A.D.; Wasan, D.T. Mechanisms of stabilization of water-in-crude oil emulsions. *Industrial and Engineering Chemistry Research* 2001, 40(14) 3009-3014

Li, H., Long, J., Xu, Z., Masliyah, J., Flocculation of kaolinite clay suspensions using a temperature-sensitive polymer. *Materials, Interfaces and Electrochemical Phenomena* 2006, 53(2) 479-488

Liu, J.; Xu, Z.; Mashliyah, J. Interaction between bitumen and fines in oil sands extraction system: Implication to bitumen recovery. *The Canadian Journal of Chemical Engineering* 2004, 82(4), 655-666

Liu, J.; Xu, Z.; Mashliyah, J. Role of fine clays in bitumen extraction from oil sands. *Materials, Interfaces, and Electrochemical Phenomena* 2004, 50(8), 1917-1927

Long, J.; Xu, Z.; Masliyah, J.H. Role of illite-illite interactions in oil sands processing. *Colloids and Surfaces A: Physicochemical and Engineering Aspects* 2006, 281(1-3) 202-214

Ma, C.; Eggleton, R.A. Cation exchange capacity of kaolinite. *Clays and Clay Minerals* 1999, 47(2) 174-180

Masliyah, J. H.; Czarnecki, J.; Xu, Z. Chapter 1, 2 in Handbook on Theory and Practice of Bitumen Recovery from Athabasca Oil Sands Volume I: Theoretical Basis. *Kingsley Knowledge Publishing* 2011

Masliyah, J.; Zhou, Z.; Xu, Z.; Czarnecki, J.; Hamza, H. Understanding water-based bitumen extraction from Athabasca oil sands. *The Canadian Journal of Chemical Engineering* 2004, 82(4), 628-654

Masliyah, J.H.; Bhattacharjee, S. Electrokinetic and Colloid Transport Phenomena. *John Wiley & Sons, Inc.* 2006

Matthews, J. Chapter 9 in Handbook on Theory and Practice of Bitumen Recovery from Athabasca Oil Sands Volume II: Industrial Practice. *Kingsley Knowledge Publishing* 2011

McLennan, J.; Deutsch, C.V. SAGD Reservoir Characterization Using Geostatistics: Application to the Athabasca Oil Sands, Alberta, Canada. Canadian Heavy Oil Association handbook, 2d ed. *Canadian Heavy Oil Association* 2005

McNeill, J. Will Alberta's oilsands tailings finally be cleaned up? (Blog Post) *Pembina Institute* 2017

Mpofu, P.; Addai-Mensah, J.; Ralston, J. Influence of hydrolyzable metal ions on the interfacial chemistry, particle interactions, and dewatering behavior of kaolinite dispersions. *Journal of Colloid and Interface Science* 2003, 261(2) 349-359

Nabzar, L.; Pefferkorn, E.; Varoqui, R. Polyacrylamide-sodium kaolinite interactions: Flocculation behavior of polymer clay suspensions. *Journal of Colloid and Interface Science* 1984, 102(2) 380-388

Nelson, S.A. Class Note (url: www.tulane.edu/~sanelson/eens1110/massmovements.htm) 2015

Ng, J.K.H. Study of thermoresponsive hybrid polymer for oil sands applications, M.Sc. thesis, University of Alberta 2018

Nusri, S.; Tan, X.; Choi, P.; Liu, Q. Using surface geopolymerization reactions to strengthen Athabasca oil sands mature fine tailings. *The Canadian Journal of Chemical Engineering* 2016, 94 1640-1647

Oil Sands Magazine: Bitumen Production Facilities. *Oil Sands Magazine* 2018 (Retrieved from www.oilsandsmagazine.com/projects/bitumen-production)

Oil Sands Magazine: Paraffinic Froth Treatment. *Oil Sands Magazine* 2018 (Retrieved from www.oilsandsmagazine.com)

Oil Sands Magazine: Tailings Ponds 101. *Oil Sands Magazine* 2018 (Retrieved from www.oilsandsmagazine.com)

One Trillion Litres of Toxic Waste and Growing: Alberta's Tailings Ponds. *Natural Resources Defense Council and Environmental Defense* 2017

Pensini, E.; Harbottle, D.; Yang, F.; Tchoukov, P.; Li, Z.; Kailey, I.; Behles, J.; Masliyah, J.; Xu, Z. Demulsification mechanism of asphaltene-stabilized water-in-oil emulsions by a polymeric ethylene oxide–propylene oxide demulsifier. *Energy and Fuels* 2014, 28(11) 6760-6771

Radler, M.; Oil, gas reserves rise as oil output declines. *Oil & Gas Journal* 2003, 107(47), 18-21

Rao, F.; Liu, Q. Froth treatment in athabasca oil sands bitumen recovery process: A review. *Energy and Fuels* 2013, 27(12), 7199-7207

Rao, F.; Liu, Q. Geopolymerization and its potential application in mine tailings consolidation: a review. *Mineral Processing and Extractive Metallurgy Review* 2015, 36(6) 399-409

Rodahl, M.; Höök, F.; Fredriksson, C.; Keller, C.A.; Krozer, A.; Brzezinski, P.; Voinova, M.; Kasemo, B. Simultaneous frequency and dissipation factor QCM measurements of biomolecular adsorption and cell adhesion. *Faraday Discussions* 1997, 107 229-246

Roiter, Y.; Jaeger, W.; Minko, S. Conformation of single polyelectrolyte chains vs. salt concentration: Effects of sample history and solid substrate. *Polymer* 2006, 47(7) 2493-2498

Romanova, U.; Yarranton, H.; Schramm, L.; Shelfantook, W. Investigation of oil sands froth treatment. *The Canadian Journal of Chemical Engineering* 2004, 82(4) 710-721

Rondon, M.; Pereira, J.C.; Bouriat, P.; Graciaa, A.; Lachaise, J.; Salager, J. Breaking of water-in-crude-oil emulsions. 2. Influence of asphaltene concentration and diluent nature on demulsifier action. *Energy and Fuels* 2008, 22(2) 702-707

Ruehrwein, R.; Ward, D. Mechanism of clay aggregation by polyelectrolytes. *Soil Science* 1952, 73(6) 485-492

Salgin, S.; Salgin, U.; Bahadir, S. Zeta potentials and isoelectric points of biomolecules: the effects of ion types and ionic strengths. *International Journal of Electrochemical Science* 2012, 7(12) 12404-12414

Sauerbrey, G. Verwendung von schwingquarzen zur wägung dünner schichten und zur mikrowägung. *Zeitschrift für Physik* 1959, 155 (2): 206–222

Scheutjens, J.M.H.M.; Fleer, G.J. Statistical theory of the adsorption of interacting chain molecules. 2. Train, loop, and tail size distribution. *The Journal of Physical Chemistry* 1980, 84(2) 178-190

Science 1952, 73(6) 485-492

Shelfantook, W. A. Perspective on the selection of froth treatment processes. *The Canadian Journal of Chemical Engineering* 2004, 82(4) 704-709

Start of Production Operations in Oil Sands Project at Hangingstone in the Province of Alberta, Canada, and Decision not to Re-Start SAGD Operations in the 3.75 Section Area. *JAPEX*, 2017.

Takamura, K. Microscopic structure of athabasca oil sand. *The Canadian Journal of Chemical Engineering* 1982, 60(4) 538-545

Tripathy, T.; Pandey, S.R.; Karmakar, N.C.; Bhagat, R.P.; Singh, R.P. Novel flocculating agent based on sodium alginate and acrylamide. *European Polymer Journal* 1999, 35(11) 2057-2072

Upstream dialogue – The facts on oil sands. *The Canadian Association of Petroleum Producers* 2014

Valapa, R.B.; Loganathan, S.; Pugazhenthi, G.; Thomas, S.; Varghese, T.O. An Overview of Polymer-Clay Nanocomposites. Chapter 2 of Clay-Polymer Nanocomposites. *Elsevier Inc*. 2017

Van de Steeg, H.G.M.; Stuart, M.A.C.; De Keizer, A.; Bijsterbosch, B.H. Polyelectrolyte adsorption: a subtle balance of forces. *Langmuir* 1992, 8(10) 2538-2546

Vedoy, D.R.; Soares, J.B.P. Water-soluble polymers for oil sands tailing treatment: A review. *The Canadian Journal of Chemical Engineering* 2015, 93(5) 888-904

Verwey, E. J. W.; Overbeek, J. Th. G. Theory of the stability of lyophobic colloids. *The Journal of Physical Chemistry* 1947, 51 (3) 631–636

Voinova, V.M., Rodahl, M., Jonson, M., Kasemo, B. Viscoelastic acoustic response of layered polymer films at fluid-solid interfaces: continuum mechanic approach. *Physica Scripta* 1999, 59(5) 391-396

Wang, C. Flocculation-Assisted Dewatering of Fluid Fine Tailings Using a Volute Screw Press. Ph.D thesis, University of Alberta 2017

Wang, C.; Han, C.; Lin, Z.; Masliyah, J.; Liu, Q.; Xu, Z. Role of preconditioning cationic zetag flocculant in enhancing mature fine tailings flocculation. *Energy & Fuels* 2016, 30(7) 5223-5231

Wang, C.; Harbottle, D.; Liu, Q.; Xu, Z. Current state of fine mineral tailings treatment: A critical review on theory and practice. *Minerals Engineering* 2014, 58 113-131

Wang, S.; Zhang, L.; Yan, B.; Xu, H.; Liu, Q.; Zeng, H. Molecular and surface interactions between polymer flocculantchitosan‑g‑polyacrylamide and kaolinite particles: Impact of salinity. *The Journal of Physical Chemistry C* 2015, 119(13) 7327-7339

Wieland, E.; Stumm, W. Dissolution kinetics of kaolinite in acidic aqueous at 25°C. *Geochimica et Cosmochimica Acta* 1992, 56(9) 3339-3355

Yan, L.; Masliyah, J.H.; Xu, Z. Understanding suspension rheology of anisotropically-charged platy minerals from direct interaction force measurement using AFM. *Current Opinion in Colloid & Interface Science* 2013, 18(2) 149-156

Yang, W.Y.; Qian, J.W.; Shen, Z.Q. A novel flocculant of $Al(OH)_3$–polyacrylamide ionic hybrid. *Journal of Colloid and Interface Science* 2004, 273(2) 400-405

Yoon, S. Membrane Bioreactor Processes: Principles and Applications. *CRC Press* 2016